FINE STRUCTURE IN THE THERMAL DENATURATION OF DNA: HIGH TEMPERATURE-RESOLUTION SPECTROPHOTOMETRIC STUDIES

Authors: **Akiyoshi Wada**
Department of Physics
University of Tokyo
Tokyo, Japan

Sadato Yabuki
Department of Physics
Gunma University
Maebashi, Japan

Yuzuru Husimi
Department of Environmental Chemistry
Saitama University
Urawa, Japan

Referee: J.G. Brahms
Biomolecular Spectroscopy Laboratory
Institute of Molecular Biology
University of Paris
Paris, France

I. INTRODUCTION

Properties of double stranded DNA are of interest to scientists in various branches: biologists, chemists, physicists, and polymer scientists. Their interests, however, are concerned with different aspects. Biologists have tried to explore the very detailed structure of the genetic information in DNA hidden behind the genetic map whose geometrical feature had already been clarified with great precision by the analysis of chromosome. Chemists and physicists on the other hand have been greatly inspired by the establishment of a model of atomic precision not only because of its fascinating structural regularity and unusual molecular properties but also because it opened a way to explore the central problem of biology from a different side of science. From there, scientists have proceeded toward the common and ultimate goal which is the elucidation of the biological functions of DNA by its chemical and physical structures.

Since the establishment of the model of the double helix, its chemical structure, the base sequence, has been correlated with the genetic information in terms of the *codon*. Although there may be many more genetic features to be disclosed in the chemical structure of DNA, such as doubly coded genetic information which has been found recently in short viral DNAs, a breakthrough in the most difficult stage has been made as far as the chemical structure is concerned.

The primary interest in the physical structure of DNA is of course the double helical folding of nucleotide chains, the so-called secondary structure. This structure is considered to have evolved so that the genetic information may be protected by an array of stable base pairs inside the double helical folding of the main chains. These closed base pairs are believed to break when reading out the genetic code. Hence the unfolding process directly relates to the genetic function; nevertheless, from a physical point of

view, it has long been studied mostly within the framework of a one-dimensional uniform lattice model, where the base sequence was not explicitly taken into consideration.

Recently remarkable developments have been achieved both in the precision of experiment and the rigor of theoretical formulation. Experimentally, the high temperature-resolution technique in the spectroscopic studies of DNA solution has disclosed much evidence of discrete unfolding of DNA in solution that is revealed as fine structures in the melting profile of relatively short DNAs. This fact, together with the evidence of electron microscopic observations, clearly indicates that the double strand consists of a series of regions with different stabilities which melt successively in a discrete and locally cooperative manner. On the other hand, in the theoretical realm, the development of a rigorous algorithm has made it possible to include the base sequence explicitly into the statistical mechanical calculation of the helix-coil transition of sequence-determined DNA molecules. The fine structure in the melting profile is elucidated in terms of the molecular structure and its internal potential energy. Needless to say, the role played by the success of the full determination of base sequences of several viral DNAs such as ϕX174 or fd phage DNA is important; without it the theoretical study of the melting of DNA might not be very different from a mathematical game. In general, the non-uniformity of the physical structure along the DNA is becoming an important subject in the study of the biological role of DNA. The palindrome in the genetic sentence discovered by the sequence analysis is one example. This kind of sequence seems to be quite favorable for the formation of hairpin loops which are made by each of the nucleotide chains of the double helix and stick out from the main body. Another important subject is polymorphism of the double helical structure; that is, beside the B form which is considered to be the stable structure in solution, the DNA may locally take A, C, or other types of double helical structures according to its local base sequence. Details of such local variety in the physical structure and their biological roles remain to be investigated in the future.

DNA is now found to have a larger variety of physical properties along its strand than its appearance indicates. Thus the melting of DNA should be considered in the final analysis to be a profound phenomenon arising from these diverse characteristics.

The current status and aims of research on DNA melting are (1) to establish higher precision and resolution in the experimental method, (2) to find better models and thermodynamic parameters for the theoretical calculation of the melting profile, (3) to establish a map of the distribution of double helix stability along the DNA, (4) to relate it with the biological function of the DNA, and (5) to find its genetic and evolutional origin. Also, a practical application of the melting technique to the genetic research on DNA, such as recombination or gene manipulation, is a highly important subject to be explored.

The present review is intended to give a systematic account of these high-resolution studies of the melting of DNA in solution by referring both to the experimental and theoretical studies which have been made during the last decade. Among the high-resolution studies, the topics on the electron microscopic observation will only be referred to briefly in the present review. This does not mean that the method is unimportant; rather it is simply because we are not experts on this technique and cannot do justice to this field. Therefore we confine ourselves to the subject of the spectroscopic observation of DNA solutions. Indeed the electron microscopic technique has extremely high positional resolution to locate the melting locus in the DNA, and is complementary to the high temperature-resolution of the spectroscopic method.

The primary aim here is to study the multimodal physical stability of the DNA double helix in connection with its chemical and genetic properties. Therefore, melting studies on RNA are not included in spite of the large volume of work already done, especially on t-RNA.

II. HISTORICAL BACKGROUND

A. Brief Survey of Early Melting Studies

The present review covers the work which has been carried out since the late 1960s, after the discovery of distinct multistep modes in the thermal denaturation of DNA manifested as a fine structure in the melting profile. It is instructive, however, to first present a brief survey of topical studies carried out before that discovery, because they furnish a solid basis for the modern high-resolution study of DNA melting. Many of the quantities to be measured and methods of measurement used in previous works remain the same in contemporary works. The main difference between the earlier and current works is the matter of temperature resolution which has been vastly improved.

The melting profile is in general a two-dimensional display which is obtained by plotting a change of some property of a DNA solution against an external variable producing the melting of the DNA such as the temperature, pH, ionic strength, or the concentration of ligand molecules. From an experimental point of view, any observable property which reveals the unfolding of the double helix into a random coil may be used as a measure of the melting. During the prefine-structure era, a wide variety of physical, chemical, and biological properties of DNA had already been studied extensively. These include, for instance, the spectroscopic, hydrodynamic, electric, calorimetric, chromatographic, and immunological properties.[1] A different viewpoint of observation reveals a different aspect of the melting process of DNA.

In the theoretical realm, where the molecular elucidation of the melting phenomena is a major aim, there are two questions to be answered: how does the double helix melt, and what aspects of the molecular process are we observing as a melting profile. For the former question, a homogeneous double-helix model whose base sequence is smeared out and characterized by an averaged base composition was examined in a theoretical framework based on an extension of Ising-chain statistics.[2-5] For the latter question, physical properties, especially spectroscopic ones, were studied most because of their clear implications with regard to the molecular structure.[2,6] Other properties, however, were also examined in detail, for they provide their own unique information about the complex processes of melting.

Thus, as far as the homogeneous model and the low-resolution melting profile are concerned, the theory accounts quite well for the experiments on homo-polynucleotides and natural DNAs, and the thermodynamic parameters, which characterize the transition of the double helix to a random coil, have been determined. Practical aspects of the melting phenomena as related to the base-sequence specificity of DNA, that is, the application to study the homology or taxonomic relation between different DNA species, were also explored in combination with the renaturation kinetics.[1,2,7-10]

B. Spectroscopic Observation

Among possible combinations of quantities and variables for a melting profile mentioned in the last section, the change in UV absorbance by elevating temperature has become the most popular one because (1) it has a straightforward relationship with the degree of melting: the helix content, (2) environmental conditions can be set with high precision, (3) the wavelength dispersion gives multifold information, and (4) the measurement is simple and reliable. Incidentally, the UV absorbance by nucleotide bases in the wavelength region around 260 nm is well known as coming from the π-π^* electronic transition in purine and pyrimidine bases. The intensity increases by about 40% by releasing the bases from their double helical stacking. The assumption of the linear relationship between this hyperchromicity and the extent of the disruption of base pairs has been found to be valid if the helical regions contain at least seven or eight residues.[11,12]

1. T_m and ΔT

The melting profile of DNA was primarily characterized by two parameters. Namely, the melting temperature (T_m) which is defined as the temperature corresponding to the midpoint of melting,[13] and the sharpness or the breadth of melting (ΔT_a^b) which is defined as the difference between the temperatures of a and b% melting.[14] In the case of a = 15.9% and b = 84.1%, the ΔT corresponds to twice the standard deviation, σ, when the distribution of the melting temperature is assumed to be Gaussian.

As a result of comparative studies of the melting temperature for DNAs of different base compositions from a variety of organisms, a linear relationship between the melting temperature and the base composition which is expressed in terms of the G + C content was discovered.[13] Then the melting temperature appears to be a valid measure of the G + C content conversely.[15-20] As for the sharpness of melting, ΔT_s^{95} has been found to be as narrow as 0.3 to 1.5°C according to the studies on homo-polynucleotides and alternating copolynucleotides.[14,21] Therefore, if some appropriate value is assumed as a universal constant for the "natural width" of the melting of a double helix having a homogeneous base sequence, the melting profile of a natural DNA provides information about the heterogeneous distribution of its nucleotide composition. Namely, if the natural width is assumed to be 0.6°C, the standard deviation for the distribution of the G + C content is $\sigma = (\Delta T_{14.1}^{85.9} - 0.6) \times 1.25$, assuming a Gaussian distribution.[14]

A large amount of comparative studies about the variation of the mean base composition and of its standard deviation have been done for DNAs of one individual or of different species. From a historical point of view, the finding of a fine structure in the melting of a single DNA has partly been made in the course of such detailed study of the heterogeneity among DNAs.

2. Effect of Salt Concentration on T_m

The solution components affecting the relationship betwen T_m and the G + C content, X_{GC}, have been studied extensively.[1] These are the ionic strength, metal ion, formaldehyde, alkylammonium ions, polyamine, polypeptide, histone, and many proteins such as RNase and DNA unwinding proteins. The effect of the ionic strength, μ, is particularly important for most of the melting experiments and is expressed quantitatively by the following equations. (See References 13 and 22 for Equation 1 and Reference 17 for Equation 2.)

$$T_m = 16.1 \log\mu + 41X_{GC} + 81.5 \quad (1)$$

$$100X_{GC} = [\tan(70.077 + 3.32 \log\mu)] \cdot (T_m - 175.95) + 260.34 \quad (2)$$

The effects of the ionic strength and of most other parameters on the melting of a whole DNA are found to be more or less similar to those of local melting produced by an internal heterogeneity as described later.

3. Asymmetry of the Melting

The melting profiles of sequence-determined oligonucleotides,[23] high molecular weight homo- or alternating co-polynucleotides[24] and bacterial DNAs[14] appeared to be unimodal and smooth when their derivatives were approximated, as a first assumption, by Gaussian distribution. In more detailed studies, however, the melting profile was in most cases found to be asymmetric to some extent.[14,25] It is found that each half of the profile, above and below T_m, is nearly perfectly Gaussian with a separate standard

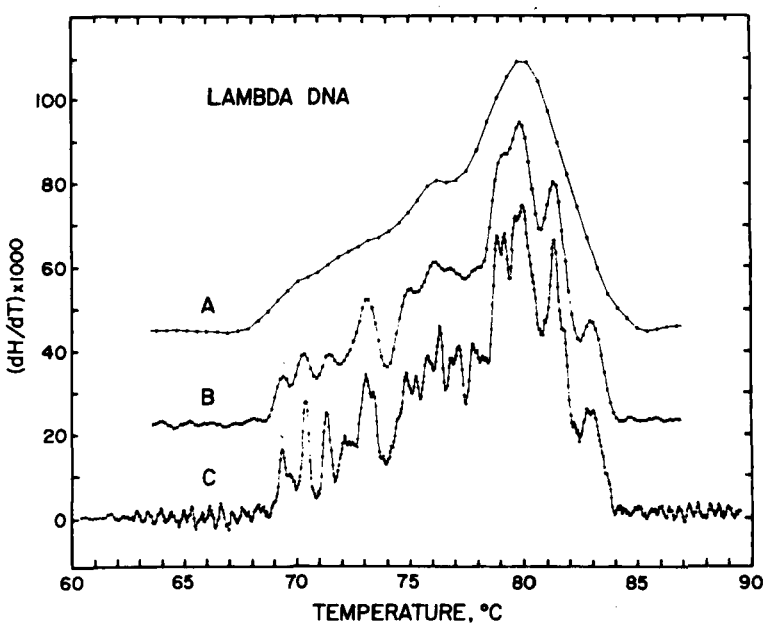

FIGURE 1. Differential melting profiles of λ-DNA with different temperature-resolutions.[34] Temperature derivative of hyperchromicity at 270 nm is plotted against temperature. Solution: 30m*M* NaCl. Temperature slit width: (A) 0.45°C, (B) 0.135°C, and (C) 0.045°C. Heating rate: 0.1°C/min. (Reprinted with permission from Vizard, D. L. and Ansevin, A. T., *Biochemistry*, 15 (4), 743, 1976. Copyright by the American Chemical Society.)

deviation, σ_{left} or σ_{right}.[14] The degree of asymmetry or skewness, which is a third parameter to describe the melting profile, is introduced and is given by $\sigma_{left}/\sigma_{right}$.[14,26] In the case of bacterial DNAs it ranges from 1.0 to 1.6 with an average of 1.33, and is little dependent upon the G + C content. On the other hand, many DNAs of higher organisms have been found to be highly asymmetric.

4. Fine Structures

A stepwise melting has been found in spectroscopic studies of some short DNAs of viral or cytoplasmic origin.[27-31] The intermediate states of DNA melting which had been found previously by electron microscopic studies[32,33] were recognized to consist of a series of many distinct steps of local melting. Today, the increased precision in the observing technique makes possible the resolution of melting steps of as many as several tens of peaks in the fine structure as shown in a typical example in Figure 1.[34] Namely, continuous plotting of the melting curve instead of point by point plotting, increased stability of spectrophotometers, and refined techniques for processing experimental data are the major factors which have improved the signal-to-noise ratio of the measurement and made the investigation of reliable melting profiles possible.

There have been many excellent review articles related to the theoretical[3-5] and experimental[1,2,35-37] aspects of the topics in the pre-fine-structure era. There are also detailed reviews on the topics of synthetic polynucleotides[38-41] and t-RNA.[42] The effects of base distribution[4,5] on the melting profile and the fine structure problem[37] have been discussed in some of these articles.

III. EXPERIMENTAL PROCEDURES

The melting curve is usually displayed by plotting the temperature derivative of the

absorbance of a DNA solution at a wavelength in the hypochromic region (dA_{260}/dT at 260 nm, for instance) against temperature. The derivative plot is done in order to make the detailed structure visually more apparent. A discrete feature in the melting process is exhibited as a series of peaks on the temperature axis. Although there is no new information added by doing so, it helps much to distinguish individual steps more clearly than in a plot of A_{260} vs. T.

The method of differentiation can be divided into two broad classes: (1) the direct measurement of the difference between the optical densities of two DNA solutions at slightly different temperatures, and (2) the numerical differentiation of an absorption-temperature curve by a computer. In either case, thorough sampling of absorbance data without loss is essential to obtain enough information density to provide an adequate signal-to-noise ratio.

A. Direct Differentiation Method

Differential melting profiles can be obtained by recording the difference in absorbance between two identical DNA solutions maintained with a small constant temperature difference.[20,43] A conventional double-beam ratio-recording spectrophotometer may be used for the measurement. The difference in absorbance is measured continuously by increasing temperature, so that a differential melting curve can be plotted directly on a recorder. The advantage of this method is its simplicity. According to Blake and Lefoley,[20] the quality of the melting profile obtained in this fashion indicates its resolution to be no worse than, and in many respects better than, that obtained by numerical differentiation. The accuracy of this method depends entirely upon the accuracy of the small constant temperature difference through the whole temperature range of observation. In one typical case,[20] the temperatures of the two samples are controlled independently by circulating water thermoregulated with a pair of modified Haake-FS baths. The temperatures are increased linearly at discrete, reproducible rates, which are adjustable between 0.1 and 1.0°C/min with a pair of step motors connected directly to the thermoregulators. Temperatures are monitored to a hundredth of a degree with a pair of thermistors calibrated to within ±0.1°C absolute, while the temperature difference is monitored continuously with a linearized differential platinum resistance bulb transmitter and a digital voltmeter. Most of the measurements were done with temperature differences of around 0.25°C; the reproducibility is found to be ±0.0001 in absorbance. Profiles plotted by this device are shown in Figures 2a and 2b.[20]

An alternative to the above method is the difference-measurement of two solutions at the same temperature but with slightly different salt concentrations.[44] This gives a small difference in their melting temperatures; thus a temperature differential curve can be obtained while maintaining two solutions at the same temperature.

B. Numerical Differentiation

Numerical differentiation is usually carried out for a set of absorbance data measured in the temperature region of interest, either by real-time data processing with an on-line computer or by an off-line process with hard-copied data which have been stored on punched paper tape or disk memory. The off-line process is advantageous in many aspects as there is freedom to select a set of optimum parameters for the curve analysis. An optimum condition depends on the mode of display of the result; for instance, whether or not temperature resolution should be given priority over signal-to-noise ratio. The mode is usually decided after the completion of an experimental run. The plots in Figure 1 exhibit the profiles obtained by numerical differentiation with three different temperature slits, which clearly give an idea about the relation between the temperature-slit width and resolving power. To obtain a melting profile

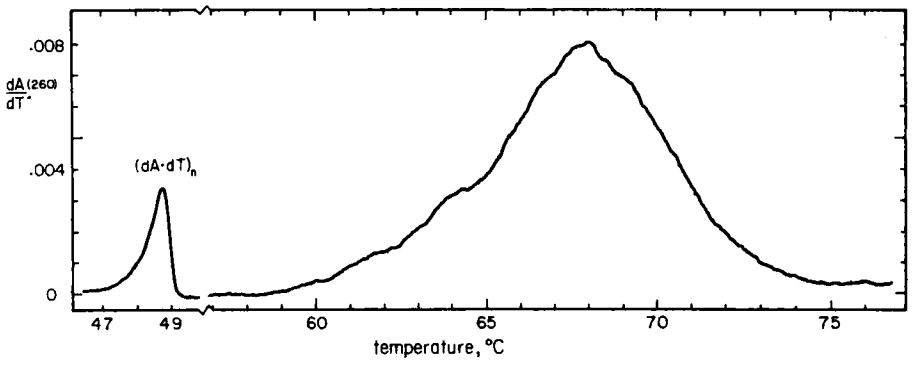

A

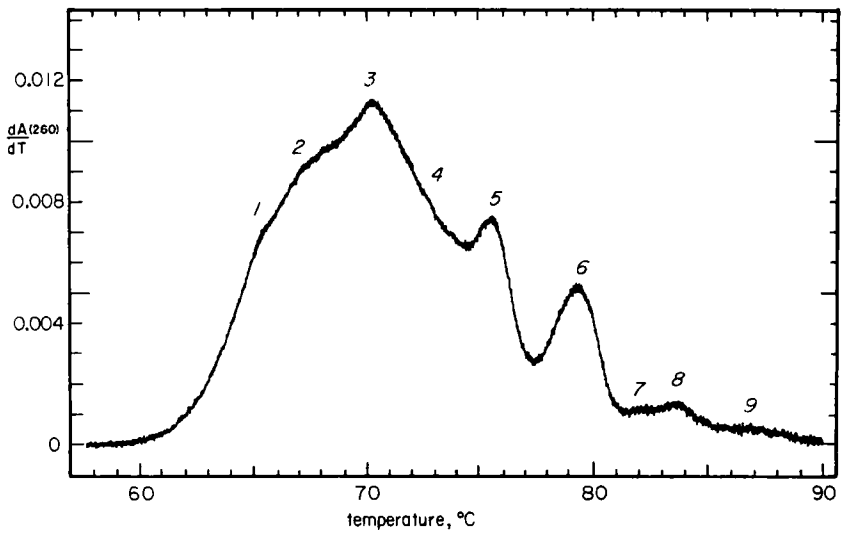

B

FIGURE 2. Differential melting profiles of (A) *B. subtilis* DNA and (B) calf thymus DNA, measured by the direct differentiation method (see text).[20] Solution: 12m*M* NaCl. Temperature difference: 0.36°C for (A) and 0.31°C for (B). Heating rate: 0.214°C/min. The spike at lower temperature in (A) is poly(dA·dT) marker that was added to the sample solution for monitoring temperature. (From Blake, R. D. and Leforey, S. T., *Biochim. Biophys. Acta*, 518, 238, 1978. With permission.)

of good quality, there are several requirements to be satisfied by the measuring apparatus and conditions, by the DNA samples and solution system, and by the procedure of data processing as detailed as follows.

1. Measuring System

The current status of the apparatus and experimenal conditions of the measuring systems which are used in several research groups are listed in Table 1. The stability of spectrometers is of the order of 10^{-4} optical density (OD) units. It is hard to say whether or not the single-beam spectrometer is more advantageous than the double-beam spectrophotometer for the present purpose, if the intensity of the light source is stable enough. The latter seems to be better at first glance, but a slight change which

Table 1
SPECIFICATIONS OF HIGH TEMPERATURE-RESOLUTION APPARATUS USED IN SEVERAL LABORATORIES

Optical axis	Temperature axis		Ref.
1. Spectrophotometer	1. Temperature elevation	1. Thermometer (°C)	
2. Stability	2. Data access: δT(degree/data)	2. Range of control (±°C)	
	3. Rate of temperature elevation: R (°C/min)	3. Fluctuation(±°C)	
1. Carry 118C double beam[a,b]	1. Continuous	1. Thermistor[d]	20
2. $\pm 3 \times 10^{-4}$ O.D.	2. Continuous	2. 0.1	
	3. 0.1 ~ 1.0	3. 0.02[a]	
1. Hitachi EPS 20	1. Continuous	1. Thermocouple	45
2. $\pm 10^{-4}$ O.D.	2. Continuous	2. —	
	3. 0.13 ~ 0.20	3. 0.10	
1. Zeiss DMR 10 single & double beam	1. Stepwise	1. Platinum wire in reference cell	46
2. $\pm 3 \sim 4 \times 10^{-4}$	2. Discrete[c]	2. —	
	3. 0.05 ~ 0.1°C/ step 1 step/1 ~ 2 min.	3. 0.01 ~ 0.001	
1. Hilger-Uvispec Cary 118XC	1. Continuous	1. Thermocouple or thermistor in sample cell	47
2. $\pm 5 \times 10^{-4}$ O.D.	2. Continuous	2. —	
	3. 0.1 ~ 0.2	3. 0.04	
1. Gilford 222 single beam	1. Continuous	1. Thermistor with linearlizer in reference cell	34,48
2. $\pm 1.4 \times 10^{-4}$ at 0 absorbance $\pm 1.7 \times 10^{-4}$ at 0.45 absorbance $\pm 2.1 \times 10^{-4}$ at 1.14 absorbance	2. Discrete: 0.045	2. 0.1	
	3. 0.10 ~ 0.2	3. 0.001	
1. Hitachi 124 double beam	1. Continuous	1. Thermistor in sample cell	49
2. $\pm 4 \times 10^{-4}$ O.D.	2. Discrete: 0.03 0.15 ~ 0.18	2. 0.1 3. 0.01	

[a] Direct differentiation. Temperature difference between two cells: 0.15 ± 0.02°C.
[b] Light source: tungsten-halogen lamp.
[c] Stepwise temperature elevation.
[d] With internal reference.

occurs in the deflection mechanism of light beams in the double-beam spectrometer sometimes produces a serious long-time drift in the light intensity which results in a spurious hump in the melting profile. The superiority of the double-beam spectrometer is evident in the case of the measurement of wavelength dispersion.

Recently a micro-spectrophotometric device was introduced by Grachev and Perel-royzen into the measurement of high resolution melting experiment.[77] The apparatus enables the measurement at several wavelengths simultaneously with 0.5 to 1 μg of DNA. A vast reduction in the volume of sample solution will greatly help the melting study where the large amount of DNA necessary for the experiment has always been an obstacle in extending the research to biologically important subjects.

Temperature measurement is usually done by using a thermoelectric sensor, the non-linearity of which is calibrated by interpolation with a polynomial function. Sometimes

it is helpful to use a synthetic polynucleotide of known T_m, such as poly rA·rU or poly dA·dT, as an internal standard to precisely monitor the melting temperature with respect to the effect of ionic strength.[20] It provides a distinguishable marker in the melting curve (as shown in Figure 2A) which gives a common origin for the temperature axes of individual measurements, where the equality of ionic strength is not always guaranteed.

There are two modes of temperature elevation currently in use: a continuous temperature elevation[34,45,48-50] and a temperature jump.[43,46,51] In the first mode the data are sampled without interruption, while in the second the attainment of equilibrium at each temperature is confirmed after each jump[46] in temperature and data taking is interrupted. The details about the merits and demerits of each of these modes of temperature elevation are a controversial matter and have been discussed elsewhere.[34,46,48,52] We, however, believe that so long as the rate of heating is slow enough compared to the conformation transition of the DNA and the time course of the absorbance change after the temperature jump is a simple monotonously decaying one, both modes should give identical results. The choice between the two modes depends on experimental conditions such as the stability of the spectrophotometer, the accuracy with which the solution temperature is maintained, and the possibility of thermal degradation of the DNA. Which of these factors is more important seems to be a matter of the personal taste of the investigator. As experimental evidence, in the case of λ DNA, the melting profiles were found to be independent of the heating rate over the range of 0.1 to 0.3°C/min (20∼30 m*M* [Na^+]).[4,49,53] This is also true for the DNAs and their fragments from ϕX174 and fd phage.[54] On the other hand, at even slower heating rates, the two melting profiles of the mitochondrial DNA from a *petit* mutant of yeast which were measured at 0.024 and 0.08°C/min (15 m*M* [Na^+]), were reported to show a slight difference especially in a higher temperature region.[46] However, the slow heating rate in this case, where the sample is eventually exposed to high temperature for a long time, might have caused a degradation of the DNA.[34] Therefore, an optimum rate of temperature elevation should be chosen that is slow enough compared to the rate of unfolding, but at the same time fast enough to avoid any possible degradation caused by high temperature. The invariance of the melting profile over a range of heating rates confirms the absence of the retarded unfolding process and degradation under these experimental conditions.[34,46,48-50,53,55]

The calibration for the thermal volume-expansion of a solution is carried out with the temperature-volume relationship of water which is expressed as a quadratic equation as follows (see Reference 56):

$$V = 0.99829 + 1.045 \times 10^{-4} \cdot T + 3.5 \times 10^{-6} \cdot T^2 \qquad (3)$$

2. DNA Samples and Solution Conditions

Purity of the DNA sample (i.e., freedom from protein contamination) is important because residual proteins, especially basic ones like histone or protamine, are known to distort the melting profile to a great extent.[1,50,57-59] Single- or double-chain scission is another factor which deforms the melting profile.[34,60,61] An end of the chain newly created by nicking or double-chain scission affects the double helix stability 200 to 300 base pairs away from it,[62] as will be described in the next section. The degradation and depurination[63-65] which may occur in the DNA at high temperature should be avoided; hence the rate of elevation of the solution temperature should be high so long as microscopic equilibrium is maintained in the unfolding process.

For monitoring the ionic strength, an internal standard is useful. This is described in the section on temperature calibration.[20]

Divalent cations and other ions which strongly bind to DNA produce unexpected effects (see the next section). Chelate agent, EDTA, is used to avoid these undesirable effects. These solution contaminants sometimes come from glassware;[66] therefore, the use of quartz or Pyrex® glassware is strongly advised especially in the case of a low-ionic strength experiment. Since Mg^{++} contamination has been found to cleave the RNA chain, precautions should also be taken in the case of DNAs.[67]

Bubble formation on the surface of the cuvette window by elevating the solution temperature is easily avoided by flushing out the air dissolved in the solution. This may be done by gently blowing helium gas prior to the measurement. Other factors to be remembered, though somewhat trivial, are dust in the solution, the effect of evaporation of the solvent, and dew condensation at the stopper which produces a refractive index fluctuation in solution.

3. Data Processing

A series of absorbance data as a function of temperature is the information primarily obtained by the measuring system, except for the direct differentiation method. For gaining an adequate signal-to-noise ratio, all information should be collected without loss. In practice, two sets of electric signals from the spectrophotometer (that is, one from the photomultiplier and the other from the thermistor bridge) are accumulated and sampled at short time intervals, δt (sec). Therefore, if the rate of temperature elevation is R (°C/sec), absorbance data in the temperature interval $R\delta t$ (°C) are plotted. Successive data points in a narrow temperature interval, the temperature slit δT (°C) (thus $\delta T/R\delta t$ = N data points), are then taken to calculate the derivative curves (see Table 1). A prime requirement for the high temperature-resolution study is a sufficient density of data points on the temperature axis. On the other hand, since the signal-to-noise ratio at each data point and the square root of its measuring time has a linearly proportional relationship, too high a data density is meaningless. An optimum interval is determined in relation to the temperature-resolving power to be attained in the experiment.

The factors in the data processing for obtaining a faithful high-resolution melting profile have been definitively examined by Ansevin et al.[48] According to their arguments, if (1) the subtransitions are symmetrical and do not overlap, (2) all transitions are described by the same, known, and general equations, and (3) data are absolutely accurate, three data points for each subtransition are enough to characterize it. If the three parameters are to be specified, the separation between data points on the temperature axis should not be greater than about three times the standard derivation σ of the narrowest subtransition to be observed, where a Gaussian function form for the subtransition peak and ideal experimental data have been assumed. Under actual experimental conditions with noises and overlappings of peaks, it is advisable to collect data points at temperature intervals of approximately $\sigma/3$.[48] The required interval is a function of the width and magnitude of the smallest subpeaks to be resolved and of the degree of overlap of adjacent peaks. Typical values of the interval of data points and the number N which have been used under the usual experimental conditions are $0.03 \sim 0.05$°C and about 10.

The data smoothing and differentiation are performed by fitting N contiguous data points to a simple polynomial by the least square method.[47-50] The first derivative of the polynomial at the central point of the group is taken as the smoothed value of the temperature differential of the melting curve at that point. The fit is repeated for each successive datum shifted by one point (or several points) until the whole profile is plotted. A quadratic or cubic function, or sometimes a linear one, is used as a fitting polynomial.

The effectiveness in smoothing random noise by this fitting procedure has been dem-

onstrated by Ansevin et al.[48] The smoothness obviously becomes better as more data points, N, are simultaneously considered and is better with a quadratic function than a cubic one, when they are compared for the same N. The distortion of the curve due to such manipulation of data has also been examined by Ansevin et al.[48] for simple step functions presenting Gaussian transitions with different widths as typical extremes of the melting curve. Attention has been given to distortion occurring at three different places: (1) the width of the peak at 60% of the maximum height, (2) the character of the two peripheral edges of a computed peak, and (3) the peak height. The results of these tests have shown that the fitting of absorbance data to a quadratic polynomial is unsatisfactory for high resolution results, while fitting with a cubic polynomial reproduces well all but the narrowest transition which is a step function in one data-point interval. The distortion in the last case comes from the effect of an edge enhancement. They concluded further that any arbitrarily narrow transition with a magnitude well above the background variation can be recognized when a five-point cubic polynomial fit is employed. In this processing technique, the number N and the interval of data points δT are the variables to obtain optimum conditions either for maximum resolution or minimum noise level.[48] This situation is demonstrated in Figure 1 which indicates the melting profiles from the same original data differently processed with several temperature-slit widths; n = 13 and δT = 0.45, 0.135, and 0.045°C.

The Fourier transform method, which has become popular in the pattern processing, is another convenient way to gain information without undesirable noise.[68] The method assumes the melting profile to be a series of Gaussian transitions which are superimposed and decomposes it into Fourier components. By the introduction of proper cut-off and filter functions, the curve smoothing is attained to obtain high-quality melting profiles.

The precision of the derivative melting curve, the fitting error, can be evaluated at every data point based on the closeness of fit of the observed values to the polynomial curves.[48] On the other hand, Pivec, Vitek, and co-workers[47,69] have introduced an error function to define the confidence level which evaluates the precision of the entire data set.

Data editing removes those occasional points which are certain to have been caused by spike noise. It is effective in improving the quality of the melting profile.[48]

IV. FINE STRUCTURE: A PHENOMENOLOGICAL DESCRIPTION

Since the establishment of the high temperature-resolution technique, considerable data on DNA melting have been accumulated. It is clear from Table 2, which lists the species of DNA for which high resolution profiles have been published, that a wide variety of DNAs from viral and bacterial DNAs to DNAs of higher plants and of mammalians have already been covered. The annual increase in the number of data, which is displayed in a differential form, is very rapid. From only five sets of data published before 1969, the number increased to 35 during the period 1970 to 1974 and exceeded 100 by the end of 1978.

A. Broad Classification of Melting Profiles

The observed profiles have unique features specific to the biological species from which DNAs come. The results on the DNA of λ phage, *B. subtilis*, and calf thymus shown in Figures 1, 2A, and 2B are but a few of such examples which show such apparent variety. Blake and Lefoley[20] have classfied the profiles into three basic types according to the size and sequence homogeneity of the DNA, namely, (1) the polyphasic melting of short homogeneous viral DNAs consisting of unique sequences, (2)

Table 2
DNAs FOR WHICH MELTING PROFILES WERE MEASURED AND DISPLAYED[a]

Phage DNA

Source		Ionic condition	Mode of display	Remarks	Ref.
		Lambda			
		10 m*M* Na^+	I		31
		10 m*M* Na^+ + 10 m*M* phosphate	D	spectral	27
		30 m*M* Na^+	D	$\lambda = 270$ nm	34
		0.01 × SSC	D	wild type	46
		0.05 × SSC	D		52
		0.01 × SSC	D	histone complex	70
Point mutant	CI and CI857s7	12 m*M* Na^+	D[b]		20
		0.01, 0.1, 1 × SSC	I	melt-refold[c]	28,29
		0.1 × SSC	D		53
		0.01, 0.1 × SSC	D		49
		19.5 m*M* Na^+, 1 m*M* phosphate	D	spectral	71
		1 m*M* ~ 195 m*M* Na^+ (citrate)	D	effect of ionic strength	72
Deletion mutant	b2	10 m*M* Na^+ + 10 m*M* phosphate	D		27
		0.1 × SSC	D		53
		19.5 m*M* Na^+ (1 m*M* phosphate)	D	spectral	71
		1 m*M* ~ 195 m*M* Na^+ (citrate)	D	effect of ionic strength	72
	b2b5	0.1 × SSC	D		53
		19.5 m*M* Na^+, (1 m*M* phosphate)	D	spectral	71
		0.01, 0.1 × SSC	D		49
	dg	10 m*M* NaCl + 10 m*M* phosphate	D		27
Fragment	*EcoR*I digest.	0.05 × SSC	D	left 40% curve resolved melt-refold[c]	52
	plac + "lac" operon		D	curve resolved	52

	ϕ80			
	0.01 × SSC	D	curve resolved	52
	10 m*M* Na^+ + 10 m*M* phosphate	D		27
	P2			
P2 and P2Hy	0.1, 1 × SSC	I	spectral	73
	P22			
	10 m*M* NaCl + 10 m*M* phosphate	D		27
	PM2			
	0.1 × SSC	D	curve resolved	52
	0.1 × SSC	D		45
	7.2 *M* $NaClO_4$	D	open and close	45
	T2			
	0.1 × SSC	D		45
	0.1 × SSC	D		74
	19.5 m*M* Na^+	D	spectral	71
	1 × SSC	D		26
	T3			
	0.1 × SSC	D		74
	10 m*M* Na^+ + 10 m*M* phosphate	D		27
	T4			
	100 m*M* phosphate	D,I		75
	1 × SSC	D,I	melt-remelt[d]	76
	T5			
	1 m*M* Na^+	D	curve resolved	52
	10 m*M* Na^+	I		31
	0.01, 0.1, 1 × SSC	I	melt-refold[e]	28
	0.1 × SSC	D		74

Table 2 (continued)
DNAs FOR WHICH MELTING PROFILES WERE MEASURED AND DISPLAYED[a]

Phage DNA (continued)

	Source	Ionic Condition	Mode of Display	Remarks	Ref.
		T7			
		0.1 × SSC	D	curve resolved	52
		0.1 × SSC	D,I	spectral microscopic	77
		0.1 × SSC	D		45
		0.1 × SSC	D		74
		0.1 × SSC	D[a]		44
		0.1 × SSC			
		10 m*M* Na^+	D,I		31
		5 m*M*, 30 m*M* Na^+	D		34
		7.2 *M* $NaClO_4$	D		45
Fragment		0.1 × SSC	D	spectral microscopic	77
		BF23			
		0.1 × SSC	D		74
		fd			
Whole RF linear	RHind II	0.1 × SSC	D		60,61
Fragment	RHind I	0.1 × SSC	D	fractionated	60,61
	RHap II	0.1 × SSC	D	fractionated	60
	RHga	0.1 × SSC	D	fractionated	61
		ΦX174			
Whole	random nicking	0.1 × SSC	D		78
		30 m*M*, 195 m*M* Na	D		79
Fragment	RHap II (Y_1 & Y_2)	0.1 × SSC	D	fractionated	80

	Adenovirus			
	0.1 × SSC	D	curve resolved	52
	SD			
	0.1 × SSC	D		45
	Rizobium phage			
	0.1 × SSC	I,D	curve resolved	81
	2C			
	Tris-NaCl 200 m*M* Na^+	I		82

Bacterial DNA

Source	Ionic Condition	Mode of Display	Remarks	Ref.
	B. Subtilis			
	12 m*M* Na^+	D*		20
	0.1 × SSC	D		45
	1 × SSC	D	fractionated	26
	D. pneumoniae			
	1 × SSC	I		28
	E. coli			
	100 m*M* phosphate + 100 m*M* Na^+	D		27
	P. mirabilis			
	100 m*M* phosphate + 100 m*M* Na^+	D		27
	V. comma			
	100 m*M* phosphate + 100 m*M* Na^+	D		27
	P. aeruginosa			
	100 m*M* phosphate + 100 m*M* Na^+	D		27

Table 2 (continued)
DNAs FOR WHICH MELTING PROFILES WERE MEASURED AND DISPLAYED[a]

Mammalian Nuclear DNA

Source	Ionic Condition	Mode of Display	Remarks	Ref.
	Calf			
Thymus	10 m*M* Na^+	I		31
	12 m*M* Na^+	D*		20
	0.1 × SSC	D		45
	1 × SSC	D,I	fractionated renaturation	25, 83 26
	Tris-NaCl 200 m*M* Na^+	I		82
	Na_2SO_4 13 m*M*, 1.58 *M*	D,I		84
Liver	0.1 × SSC			85
	Rat			
Thymus	low ion, + urea	D,I	histone binding	50
Liver	low ion	D	chromatin effect of heparin 5M urea	86
	0.1 × SSC	I		87
	0.1 × SSC	I		85
	Guinea pig			
Liver	0.1 × SSC	D		85
	Hedgehog			
Liver	0.1 × SSC	D		85
	Human			
Liver	0.1 × SSC	D		85
	Makakus rhesus			
Liver	0.1 × SSC	D		85

		Mouse			
Liver		0.1 × SSC	D		85
		Rabbit			
Liver		0.1 × SSC	D		85
		Dog			
Liver		0.1 × SSC	D		85
		Cat			
Liver		0.1 × SSC	D		85
		Roe deer			
Liver		0.1 × SSC	D		85
		Pig			
Liver		0.1 × SSC	D		85
		Higher Plant DNA			
		Maize			
		0.1, 1 × SSC	D		69
		Potato			
		0.1, 1 × SSC	D		69
		Pea			
		0.1, 1 × SSC	D		47,69
		S. tuberosum			
		0.1, 1 × SSC	D	fractionated	69
		Wheat			
	nuclear	0.1 × SSC	D,I	fractionated	88
		Spanish beans			
		Tris-NaCl 200 m*M* Na	I	fractionated	82

Table 2 (continued)
DNAs FOR WHICH MELTING PROFILES WERE MEASURED AND DISPLAYED[a]

Cytoplasmic DNA, Genetic Units, and Other DNA

Source		Ionic Condition	Mode of Display	Remarks	Ref.
		Mitochondria			
Yeast	ϱ^+	100 m*M* Na^+	D		89
		150 m*M* Na^+	D	melt-remelt[d]	90
		1 × SSC	D,I		30
	ϱ^-	15 m*M* Na^+	D		46
		15 m*M* Na^+	D		91,92
		0.1 × SSC	D	melt-refold[c]	51
		100 m*M* Na^+	D	mutants	89
		150 m*M* Na^+	D	mutants melt-remelt[d]	90,93
		1 × SSC	D,I		30
Rat	Liver	0.1 × SSC	D		87,94
		0.1 *M* phosphate	D,I		75
Mouse	Liver	0.1 *M* phosphate	D,I		75
Guinea pig	Liver	0.1 *M* phosphate	D,I		75
Chicken	Liver	0.1 *M* phosphate	D,I		75
Xenopus	*laevis*	120 m*M* phosphate	D,I	melt-remelt[d] cross refold-melt	95
	mulleri	120 m*M* phosphate	D,I	melt-remelt[d] cross refold-melt	95
		Chloroplast			
Chlamidomonus		1 × SSC	D,I	melt-remelt[d]	76
		Plasmid			
Colicin EI		0.1 × SSC	D	melt-refold[c]	96
pNTI		0.1 × SSC	D	melt-refold[c]	96

		Satellite			
Crab		100 m*M* phosphate	D		30
		100 m*M* Na + 50 m*M* cacodylate	I		97
Calf	Thymus	100 m*M* Na + 50 m*M* cacodylate	I		97
	Restriction fragments *EcoRI, AluI*	0.05 × SSC	D		98
Rodent		40 m*M* K^+	I	4 species	99
		Ribosomal DNA			
X. laevis		0.1 × SSC	I		100,101
X. mulleri		0.1 × SSC	I		100,101
Tetrahymena		0.1 × SSC	D,I		102
		Histone gene DNA			
Sea urchin		0.1 × SSC	I		103
		Potato tuber sprout			
		1 × SSC	D		26
		Physarum polycephlam			
		0.1 × SSC	D		52
		Kinetoplast			
Tripanosoma		1 × SSC	I	fractionated	104
		0.1 × SSC	D	melt-remelt[d]	105
		Lymphocyte			
Human		1 × SSC	D		26

[a] The wavelength for measurement is 260 nm unless otherwise stated.
[b] D: derivative plot; D*: direct differentiation; I: integrated.
[c] Melt-refold: refolding process is investigated in addition to the melting.
[d] Melt-remelt: melting profile of refolded chain is studied in addition to the melting process.

the smooth and monotonic melting of bacterial and large viral DNAs, and (3) the broad melting profile with polyphasic structure, which is observed in DNAs from higher eukaryote. Similarly, Frank-Kamenetskii, Lyubchenko, Lazurkin, and coworkers[37,45] have broadly classified the melting of naturally occuring DNAs into two categories by the type of their base sequence; that is, quasi-random or block sequence. The former type is defined as a sequence whose thermodynamic and other physical properties do not differ much from those of the true random sequence. Several virulent bacteriophages such as, T_2, T_4, T_5, and T_7 belong to this category. The homogeneity in the base distribution of these DNAs is indicated by the formation of a clearly defined layer corresponding to the uniformity of buoyant densities of their fragments in density gradient centrifugation. The melting of these DNAs takes place within a narrow temperature range, 2 to 4°C, while it is still accompanied by fine structures as a superimposed ripple.

The ripples appear to be separated as several distinct peaks if a very short DNA with 1000 or so bases is observed. For instance, the base sequences of the fragments of ϕX174 DNA, Y_1 (2745 base pairs) and Y_2 (1690 base pairs), obtained by site-specific digestion with restriction endonuclease *Hap* II, are found to be random as far as the nearest-neighbor frequency, autocorrelation of the base sequence, and the binomial distribution of the G + C content (see Section VI) are concerned.[80,106] The fragments show clear steps in their melting,[80] which indicates that a single stretch of the quasi-random sequence still results in a fine structured melting profile.[45,80,107,108]

On the other hand, the block sequence means a series of fairly long regions of several thousand base pairs, each of which has the quasi-random sequence mentioned above. DNAs of temperate bacteriophages and bacteria have been known to have such a heterogeneous distribution of blocks of quasi-random sequences with different G + C contents.[109,110] These block-wise sequences produce a polyphasic melting curve in relatively short DNAs, which is detectable even with a low-resolution experiment, as first observed by Falkow and Cowie[27] and Yabuki et al.[28] Such curves that have many peaks will tend to become smooth and monotonic as the observed DNA becomes long, because too many subtransitions are statistically averaged so as to give a smooth envelope. This was shown in the case of a long viral DNA such as that of T_2 or a bacterial DNA,[20,45] although higher resolution experiments can still detect a clear and reproducible fine structure in the former DNA.[71,74]

The peaks which appear distinctly in the melting of DNAs of higher organisms are not the product of subtransitions due to the internal heterogeneity resulting from a random fluctuation of base sequences; the DNAs seem to be too long to exhibit even small ripples on the melting envelope. Peaks may, however, come from some special families such as a satellite DNA or some other regions specific to functions of higher organisms. In most cases, peaks appear on the higher temperature side of the main melting band,[85] representing some GC-rich segments. It is quite plausible that these satellite peaks come, at least in part, from repeated sequences,[20,85] as has already been shown in some DNAs whose fragments were separated by preparative density-gradient ultracentrifugation; the fragments have been shown to have a high rate of renaturation specific to the repeated sequence.[111,112]

B. Aim of the Melting Study

The aim of research on the melting of DNA is twofold. One is the study of the phenomenon itself in which one seeks to correlate its complex feature with molecular thermodynamic processes intrinsic to the base sequence, and further, to the genetic function. Another is to look for ways to apply this highly informative and quantitative evidence of "melting spectra" to the study of biological or genetic mechanisms, just like the important role played by the atomic spectra in disclosing the atomic structure in the early days of atomic physics.

We shall, in this section, confine ourselves to itemizing several distinctive features in the melting profiles and external factors affecting them. The phenomenological characteristics will then be elucidated in terms of the base sequence in Section VI.

C. Characteristics of Subtransition

1. Line Width and Shape

The improved temperature resolution of modern apparatus and a proper selection of DNA samples have made it possible to obtain a differential melting profile as a group of sharp individual peaks corresponding to discrete local meltings.[20,34,45,46,49,52,53,60,61,71] The apparent line width ranges fom 0.2 to 1.0°C. A detailed analysis by Vizard and Ansevin[34] with the histogram of the frequency distribution of the line widths observed with the λ-phage DNA indicates that wider peaks ($2\sigma > 1.43$°C) may come from an accidental overlap of peaks. Excluding these wider peaks, they estimated the mean width of the resolved peaks to be 0.33°C, and the standard deviation of the width distribution to be .054°C.[34]

The line width is invariant regardless of the line position, that is, the melting temperature of the line. Further analysis showed that individual peaks are Gaussian[34,52] in form as expressed by $dA/dT \propto \exp -(T-T_m)^2/2\sigma^2$, where A and T_m are the absorbance and the melting tempeature of a peak, T is the temperature, and σ is the standard deviation, also used as the line width.

2. Length of Local Melting Region

The length of a unit melting region corresponding to a single peak can be estimated to be the total length of the DNA × (area under the peak/total area of the melting profile). However, the hyperchromicity at the 260 nm wavelength, which gives a maximum absorbance and is customarily used as a measure of the degree of unfolding, is not the same for the AT and GC base pairs: the degree of unfolding of AT pairs appears much more pronounced than that of GC pairs at this wavelength. In this respect, the use of the 270 nm wavelength has been recommended as an ideal wavelength at which the melting profile gives the fractional length of the melting region.[34] Alternatively, one may obtain the unbiased hyperchromicity of a peak by a linear interpolation from the values of the hyperchromicity of the GC and AT pairs. In this case, the G + C content of the melting region should be estimated in reference to the melting temperature of the peak.[29] Strictly speaking, the true local G + C content may deviate to some extent from the linear Tm − (G + C content) relationship. The error due to this, however, should not exceed the experimental precision in most of the cases.[71]

The length of a unit melting region which appears as a single peak is found to range from 300 to 1500 base pairs in the restriction fragments of the DNA of ϕX174. It ranges from 100 to 1100 in the DNA of fd phage,[61] and from 200[34] ∼ 500[49] to 1500[49] ∼ 3000[34] in the DNA of λ phage.

3. Wavelength Dispersion

Each of the disruptions of the GC and AT base pairs accompanied by the unfolding of the double helical structure produces different spectral changes in the UV region.[113-115] Utilizing this wavelength-dispersion effect of hyperchromicity, Hirschman, and co-workers[116] found biphasic characteristics in the melting of the λ-phage DNA.

Akiyama et al.[71] carried out a similar investigation on each individual peak in the melting profile of the same DNA by scanning rapidly and repeatedly over four wavelengths, 250, 260, 270, and 280 nm, during the course of the slow elevation of the temperature. Using the wavelength-dispersion data obtained by Hirschman and Felsenfeld,[117] the melting profiles corresponding to each of the disruptions of AT and GC pairs were separately plotted. Since the calculation was done within the framework of the two-term analysis by Felsenfeld and Hirschman,[115] the hyperchromic effect due to

the disruption of the stacking of unequal bases, AT and GC, is equally divided into each melting profile. These profiles clearly show that melting starts from AT-rich regions and propagates to more GC-rich regions. The positions of the corresponding peaks in the two melting curves agree quite well. Hence the melting process appearing as a single peak is a cooperative one. Thus the melting unit can be defined by its molecular characteristic as a *cooperatively melting region,* rather than by its phenomenological behavior. The base composition thus obtained spectroscopically of each individual peak can be compared with the melting temperature of the corresponding peak. The result indicates that the linear relationship between the G + C content and Tm, which was originally obtained for the melting of the whole DNA by Marmur and Doty,[13] also holds in the case of local melting within the precision of the measurement: ±1% in th G + C content. The correlation diagram between the fractions of melted GC and AT pairs becomes multiphasic instead of biphasic as obtained by Hirschman et al.[116]

Blake and Leforey[20] examined the spectroscopic dispersion for eight bacterial and three vertebrate DNAs by their direct differential method. Two wavelengths, 282 and 260 nm, were chosen for the measurement because the former had been found to be isosbestic for the disruption of AT pairs, while the latter had given the largest absorbance change when disrupted. The results also proved that a Marmur-Doty-like relationship which is quadratic in the melting temperature fits the data well, and can be applied to both whole and local melting.

It must be noted that both of these wavelength-dispersion experiments were done with a limited precision and with solutions having medium salt concentration, 10 ∼ 20 m*M* [Na^+]. At lower ionic concentration, where melting becomes highly cooperative, some of the melting peaks do not shift as a whole by ionic strength.[34,79,118,119] This evidence that the fine structure profile is ionic-strength-dependent indicates that the local T_m is not exclusively determined by the local G + C content. According to systematic investigation with a variety of synthetic polynucleotides having simply repeated patterns of 1 to 3 bases, DNAs which have the same base composition but different nucleotide sequences do not show identical melting behavior.[74,120,121] It was also shown empirically that a double helix containing both purine and pyrimidine on each of the complementary strands is more stable than the one containing only purines on one complementary strand and only pyrimidines on the other.[120] One of the few exceptions to this empirical rule is that of poly dA·dT, which is more stable than poly d(AT)·d(AT).[74,120,121]

4. *Effect of Ionic Strength*

The melting temperature of synthetic polynucleotides and the natural DNA having a sharp melting curve depends linearly upon logarithm of ionic strength, as expressed in Equations 1 and 2, in the case of aqueous solutions of weakly interacting monovalent ions such as Na^+ or K^+.[17,22,72,74,120,122-126] This is also true for DNAs which have a multiphasic melting profile,[72,74] if the T_m is defined as the first moment of the melting profile.* With this definition the linear dependency has a slope $\delta T_m/\delta \log [Na^+] =$

* T_m[26,72,74,90,113] and ΔT[72,74] of a multiphasic transition are uniquely defined as follows

$$\overline{Tm} = \sum_{k=1}^{n-1} t_k (A_{k+1} - A_k)/(A_n - A_1)$$

$$\overline{\Delta T} = [\sum_{k=1}^{n-1} (t_k - \overline{Tm})^2 (A_{k+1} - A_k)/(A_n - A_1)]^{1/2}$$

where $t_k = (T_k + T_{k+1})/2$, and A_k and T_k are the absorbance and the temperature at the k-th data point. Summations are taken for the data points covering all the melting profile. According to these definitions, $\overline{T_m}$ and $\overline{\Delta T}$ have a definite meaning as the average and the second moment of the distribution of the melting temperatures.

16.7°C in a higher concentration of [Na^+]>6.8 mM, but the slope abruptly changes to a steeper one $\delta T_m/\delta \log [Na^+]$ = 26.6°C at 4.4 mM [Na^+];[72,74] DNAs seem to have different modes of melting in an extremely low salt concentration region.[72,74,124] On the other hand, the width of a whole melting curve does not change from 5×10^{-4} to 10^{-1} M [Na^+] in the case of a relatively narrow band manifested by T7 DNA.[66] For a DNA having a multimodal melting, the width $\overline{\Delta T}$ defined above depends little on salt concentration.[49,66] In the case of λ DNA, it is in the range of 7.83 ± 0.19°C from 1.8 mM to 19.5 mM [Na^+].[49,74] $\overline{\Delta T}$ becomes narrower both above and below this concentration range.

As for the fine structure, its general feature is well retained at the relatively high salt concentration range from 10 mM to 195 mM [Na^+],[72,74] but a remarkable change is observed in the profile below 10 mM [Na^+].[34,74] The cooperativity in the transition from a double helix to a random coil is intensified by decreasing ionic strength, because the shielding effect by ionic clouds weakens. Such increase in the cooperativity is exhibited experimentally in the melting of synthetic polynucleotide.[21,24,126,128-132] The effect is especially remarkable in the case of alternating copolynucleotides such as poly d(A-T) poly d(A-T)[133] and poly d(I-C) poly d(I-C).[120] In the latter case the width increases 2.5-fold over a 100-fold increase in salt concentration.[120] The width of individual peaks in the fine structure, however, does not seem to be much affected by the change in ionic strength.[34,72,118]

Tachibana et al.[118] examined the effect of ionic strength on the restriction fragments, Y_1 and Y_2, of the DNA of ϕX174. Study on these short and sequence-determined fragments was done by resolving the components in the fine structures by the curve-resolving technique for the melting profiles at seven ionic strengths from 2.3 to 195 mM (Figure 3). The change in the position and shape of peaks by changing ionic strength was followed in terms of their local melting temperature, area, and width: T_{mi} A_i, and σ_i for the i-th peak (Figure 4). The results were analyzed by comparing them with the melting maps at higher ionic strength which were estimated with the known base sequence of the fragments and appropriate thermodynamic parameters. From these analyses the following conclusions have been drawn:

1. Averaged T_m for the whole melting profile shifts to lower temperature in accordance with the Marmur-Doty relationship; however, the shift of the melting temperature which corresponds to the subtransition of a helical region to an internal loop is relatively small compared to that of an end coil. In other words, the peak produced by loop formation moves to the higher temperature side relative to that produced by end-coil formation. The amount of this shift can be elucidated by the polyelectrolytic effect of the loop introduced by Gotoh et al.[72]
2. There are no essential changes in the location of these cooperatively melting regions and in the boundaries between them in the salt concentration range from 195 to 6 mM.
3. Below 6 mM, a drastic change occurs in the melting profiles mainly because the loop formation is suppressed so that the region which has melted as a loop forms an end coil in the melting process.
4. The width of the whole melting profile, $\overline{\Delta T}$, is almost unchanged between 195 to 6 mM but tends to become narrow on both sides of this region, as Gotoh has observed in the case of λ-phage DNA.[72]
5. The widths of individual peaks are not a strong function of salt concentration, but show a moderate decrease as the ionic concentration decreases.[34,72,79,127] This is similar to the case of homogeneous polynucleotides and is almost the same in the case of longer DNAs.

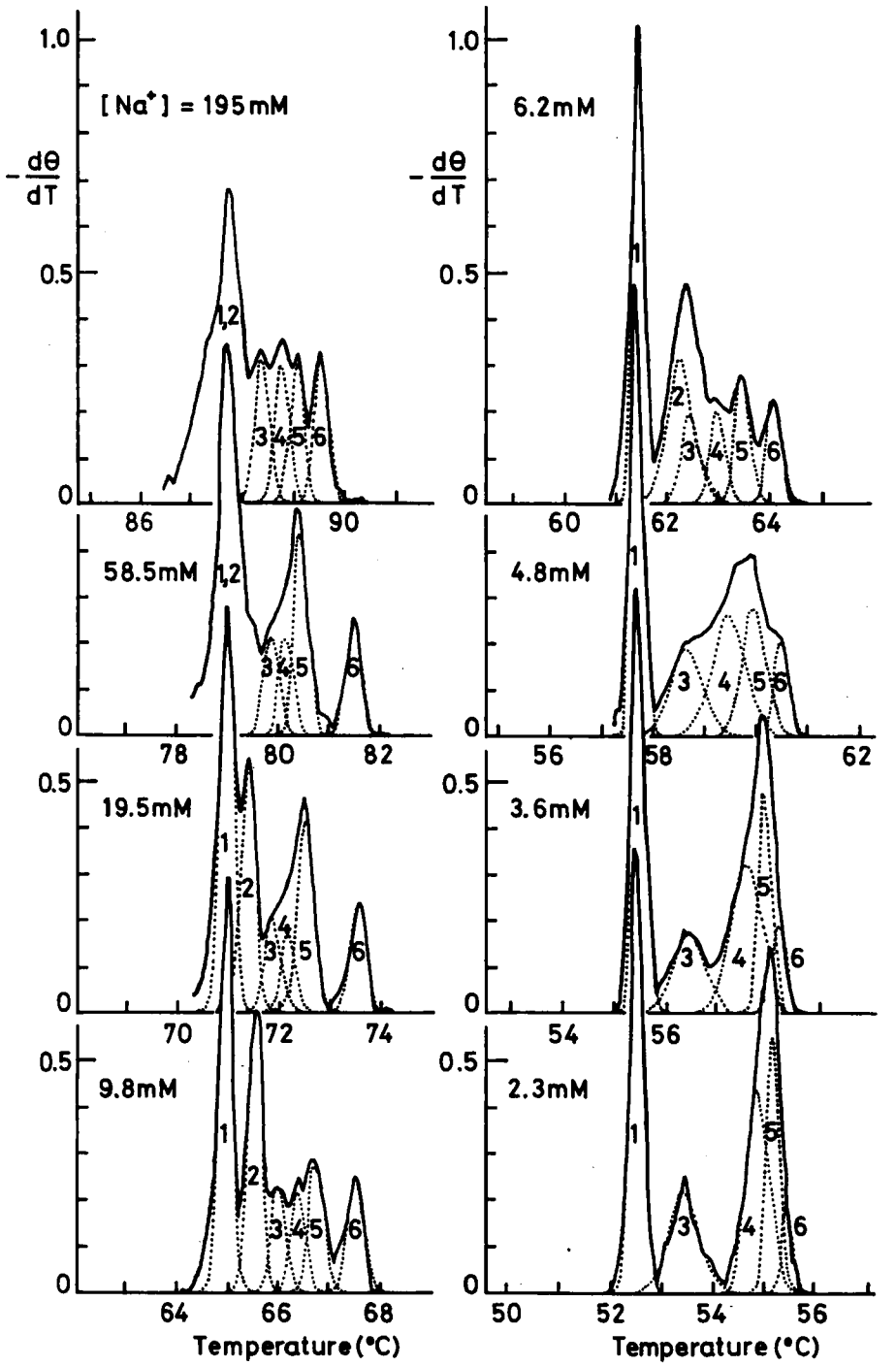

FIGURE 3. Effect of ionic concentration upon the melting fine structure of Y_1 fragment of ϕX174 DNA.[118] Dotted lines indicate individual melting peaks obtained by a curve resolving technique. Peaks 1 and 2 were not successfully separated at [Na^+] = 195 and 58.5 m*M*. Peak 2 disappears at [Na^+] ≤ 4.8 m*M* and probably merges into peak 4.

In the case of λ-phage DNA, the general feature of the fine-structure change with ionic concentration shows a clear distinction on both sides of the boundary lying at

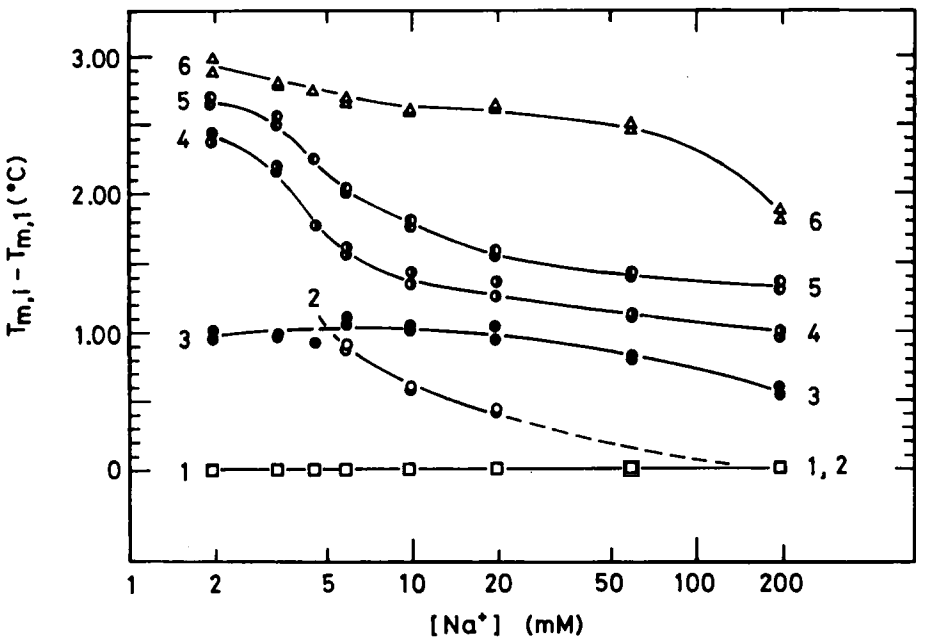

FIGURE 4. Ionic concentration dependency of melting temperatures of the peaks resolved in Figure 3.[118]

about 10 mM[72] ∿ 80 mM [Na^+].[119] The peaks which characterize the melting profile are well retained in terms of their relative positions at relatively high salt concentrations [Na^+] = 10 mM[72] ∿ 200 mM.[119] The shift of each peak can be followed and evaluated as varying between 18.4 and 15.7°C per decade of Na^+ with an inverse dependence on the local base composition of the melting segment.[119] The profile sharply changes with salt concentration below 10 mM [Na^+][72] and becomes comparatively featureless.[119] In the low salt range, 7 mM ∿ 12 mM [Na^+], as the ionic concentration increases, at least three sorts of change can be detected:[119] many peaks increase or decrease in area. This change is gradual in some cases, but may be discontinuous to show a sudden appearance of a peak within a narrow ionic concentration range. For the few peaks whose T_{mi} can be followed with the change of ionic concentration, their shifts are found to occur in parallel.[119] On the other hand, other peaks tend to coalesce at Na^+ = 6.8 mM, and then become separate again below 4.4 mM.[72] However, the profile is greatly altered with respect to the size and the position of constituting peaks.[72]

Gotoh et al.[72] compared the melting profile of the wild-type DNA of λ phage with that of b2 deletion mutant, and found that a large peak suddenly appears by the deletion in the latter DNA at a salt concentration of 2.8 mM [Na^+]. They also found in comparative studies with deletion mutants that, in the low ionic strength region, the melting of λ DNA starts from its right end rather than the most AT-rich central region.[72] This evidence may give a clue to resolving the contradiction which has arisen between two electron microscopic pictures of partially unfolded λ DNAs which are quenched differently. Namely, by quenching with formaldehyde the DNA was found to melt from a most AT-rich part in the middle of the molecule,[32,33] while the quenching of the intermediate state with low-ionic strength showed an unfolding from the end.[134] The difference may be elucidated in terms of the difference of the cooperativity which is known to decrease with formaldehyde but increase with lowering ionic strength.[72]

All of the experimental facts mentioned above are accounted for by a drastic change

in loop size which occurs in relation to the weakening of the Debye-Hückel-type electrostatic shielding with decreasing concentration of counter ions. The apparent effects of the loop and of the molecular end may not be so strong that they result in a substantial change of the melting profile in the range of 10 mM < [Na^+] < 200 mM.[72] Below 10 mM, however, the sequence order of the cooperatively melting regions seems to be rearranged due to the end and loop entropy effect.[72]

5. Effects of Other Solution Factors

a. pH

The T_m of DNA has been known not to be affected too much by a change in pH between 5.5 to 8.5.[1,122] This is also true for the fine structure. There is no important variation appearing in the melting profile over the pH range of 5 to 10.[34,135]

b. Metal Ions

Effects of many metal ions on the melting profile have been found to be more than the simple Debye-Hückel-type shielding effect. Many divalent cations, such as Ca^{2+}, Sr^{2+}, Ba^{2+}, Mn^{2+}, Ni^{2+}, Fe^{2+}, Zn^{2+}, and Mg^{2+} have a much stronger potential to effect an increase in T_m than expected from their ionic strength.[1,35,136-138] Ag^+ binds specifically to GC pairs and stabilizes them.[139,140] Cu^{2+} binds also to GC pairs, stabilizes them with a low degree of binding (r < 0.8),* but tends to destabilize with a high degree of binding (r < 0.8).[136,141,142] The effect of Hg^{2+} on T_m is also dual. It decreases T_m in a low binding region (r < 0.075), but acts to increase T_m under a high binding condition (r > 0.075).[143]

For the subtransition peaks, these metal ions work almost in the same manner that affects the local stability with respect to the local G + C content.[144] The evidence seems to be natural from the short-range character of the interactions of these ions; for instance, in the case of λ-phage DNA, the Ag^+ ion shifts G + C-rich peaks to higher temperature about 10°C from r = 0 to r = 0.05, while it shifts the peak of the lowest T_m by only 2°C. On the other hand, the effect of Hg^{2+} appears much more strongly on AT-rich peaks in the low T_m region than GC-rich peaks.[144] All such behavior of fine-structure peaks seems to be consistent when the interaction is assumed to be confined locally to within one to several bases.

c. Tetraalkyl Ammonium Ion

The tetraalkyl ammonium ion is a reagent with an interesting characteristic which alters the relative stability of base pairs $T_{mGC} - T_{mAT}$.[145] It eliminates and even reverses the stability superiority of GC pairs over AT.

The multimodal melting profile of the λ-phage DNA shrinks along the temperature axis by increasing the concentration of tetraethyl ammonium chloride (TEA). The width, $\overline{\Delta T}$, is greatly reduced from 8.35°C (0.02 M) and 5.32°C (0.20 M) to 2.43°C (1.33 M), and finally becomes a very sharp single peak with a width of 0.89°C at 2.07 M TEA,[144] while the $\overline{\Delta T}$ in 0.1 × SSC** is 9.33°C. The change of melting peaks does not, however, proceed in parallel but profiles are altered to some extent. This nonparallel shift originates from the fact that the TEA alters the thermodynamic balance, which has produced a unique melting profile, between the helix-coil boundary tension and the base stabilities represented by $T_{mGC} - T_{mAT}$.[146-148] Azbel has presented an interesting idea to utilize this effect for the analysis of the base distribution in DNA.[146-148]

* r = [metal ion] / [DNA phosphate].

** Standard saline citrate.

d. Formamide

Formamide has been known and used as a reagent to depress the melting temperature and broaden the melting width of the DNA.[149] The $\overline{T}_m$ of the λ-phage DNA decreases with formamide concentration at a rate of 0.60°C/1% formamide under an ionic condition of 0.1 × SSC.[118] In a solution of 90% formamide, ΔT increases as much as twice that without formamide. At the same time, subpeaks split and the number of peaks increases about three times the original number.[118] The results indicate that the action of formamide is dual, that is, the expansion of the temperature axis by increasing the difference in the base stability, $T_{mGC}-T_{mAT}$, and the suppression of cooperativity.

6. Additivity of Fine Structure: Effect of Chain End

The highly site-specific nature of the action of restriction endonucleases has provided an opportunity to examine and compare the melting profiles of a DNA and its fragmented pieces having definite base sequences. The melting profiles of the linear replicative form (RFIII) DNA of fd-phage (6389 base pairs) and its fragments in the digestion sets, which were obtained by the restriction endonucleases, R. *HinH* I, R. *Hga*, and R. *Hap* II were investigated.[60,61] The lack of additivity between the fragments to reproduce the melting profile of the whole DNA from which they have been fragmented is observed[60,61] (Figure 5).

Tachibana et al.[61] compared the profiles among different sets of restriction fragments in order to reconstruct the original order of arrangement of the cooperatively melting regions on the whole DNA and to make clear the effect of the cleavage end on the double helical stability. The experimental results are consistently elucidated by assuming that the end effect is not extended beyond 200 or so base pairs except for a few cases where internal loop formation occurs.[61,62] The relatively localized nature of the end effect upon the helical stability makes it possible to map the location of cooperatively melting regions by comparing the melting profiles of different sets of fragments by restriction endonucleases with different specificities.[61]

D. Observation Other Than Absorbance

The study on the fine structure of a melting profile by observing physical quantities other than optical absorbance has been limited probably because of the difficulty of gaining a sufficiently high signal-to-noise ratio. There are several articles reporting on the structure (but not its finer details) of a melting profile by calorimetric,[84] light scattering,[150] polarographic,[151] chromatographic,[152] and circular dichroic[153] measurements. Among these quantities the circular dichroism should be very promising, for it provides enough information complementary to the absorption measurement.

V. REFOLDING

Refolding of two single nucleotide chains which are complementary to each other starts with nucleation by forming a short helical stretch in register and proceeds by the zippering-up process to complete the double helical structure. The former process is slow so that the rate of the refolding is determined by this step.[8,154-156] This basic picture is also accepted as true in the case of local refolding of a partially unfolded region in the DNA. Namely, an end coil or internal looped coil refolds from its helical end or ends by the zippering process. When the local G + C content fluctuates considerably, however, local nucleation in the looped region is sometimes necessary to start the refolding. One example is the case where a GC-rich region which has melted at a temperature T_2 is sandwiched by two AT-rich regions which have melted at another temperature T_1 ($<T_2$). The melting proceeds in two steps at T_1 and T_2 with elevating

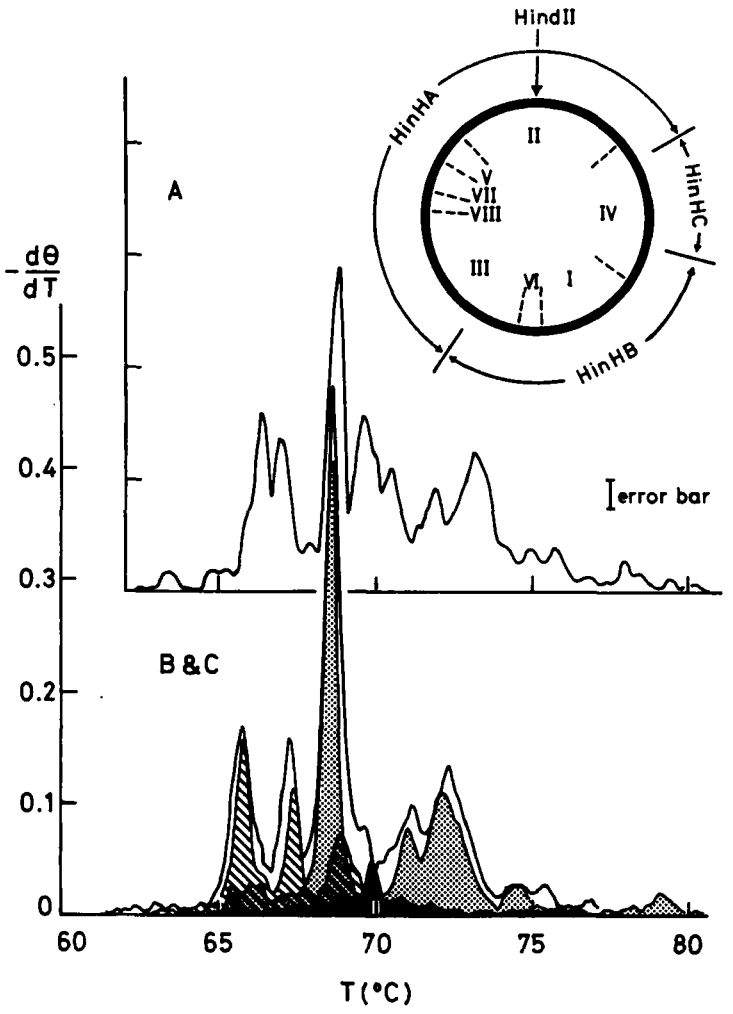

FIGURE 5. The melting profile of whole DNA is not the simple sum of those of its fragments.[60] (A) whole DNA (RF-linear) of fd phage. (B) mixture of restriction fragments: HinHA + HinHB + HinHC (bold solid line). (C) separated fragments : HinHA(⊘), HinHB (⊗), and HinHC (●). Solution: 0.1 × SSC. The melting profile of mixed fragments is found to be reproduced by the simple sum of the profiles of the fragments, but this is not the case for the whole DNA. The region in the DNA covered by each fragment is indicated at top right together with an approximate location and size of fd genes. (Roman numerals indicate the gene number.)

temperature. On the contrary, in the refolding process from a higher temperature $T > T_2$ to a temperature below T_2, the GC-rich region remains as a part of the internal loop, which is a melted stretch including the GC-rich region and the adjoining AT-rich regions. The GC-rich region does not refold during the temperature interval $T_1 < T < T_2$ because of the slow nucleation process. Below the temperature T_1, a whole loop may refold at once by the zippering process from the stable helical ends where AT-rich regions are attached. The irreversible pathway mentioned above is illustrated together with a profile of hysteresis in Figure 6. This process originating in the heterogeneity of the base sequence has been called the hysteresis of DNA melting.[29,51,96,156,157]

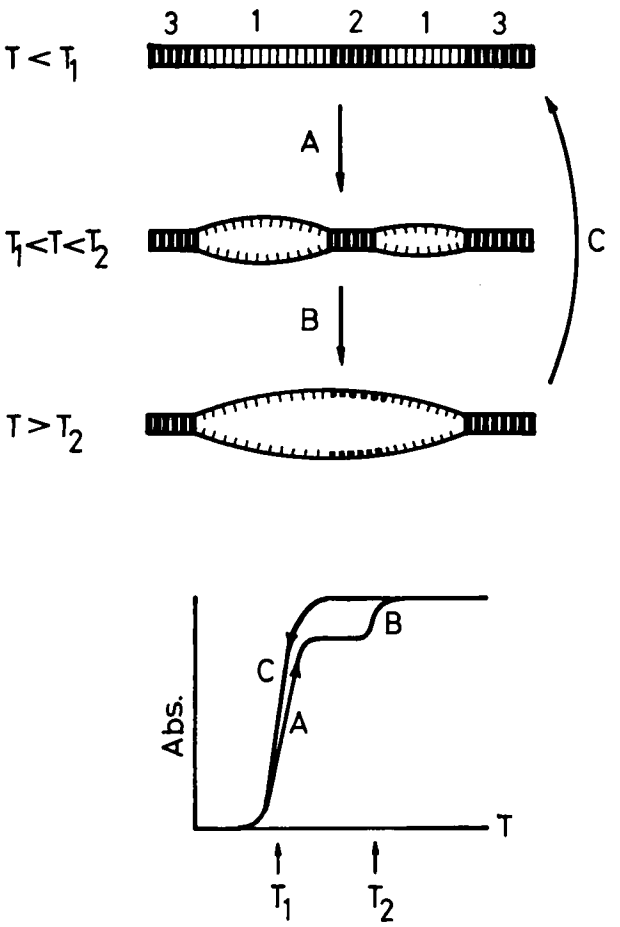

FIGURE 6. A diagram indicating melting and refolding pathways of a DNA. The local GC-rich region (region 2) is left unfolded in a large loop until AT-rich regions (regions 1) sandwiching it refold from stable helical ends of regions 3. The steps in the melting and refolding profiles shown below are in the alphabetical order as indicated.

Another but rather exceptional case which exhibits the hysteresis phenomenon occurs in relation to the intrastrand hairpin-loop formation.[158] For instance, an alternating copolymer like poly d(AT) will make hairpin loops in each of two unfolded chains in the course of refolding. If such hairpin-loop formation in both strands occurs independently, the formation of a complete helix is prevented so that the hysteresis may result. This kind of hysteresis origin may be expected in natural DNA with a repeated sequence, the palindrome, or the intergenic space sequence. On the other hand, an incomplete recovery of hypochromicity is often observed by cooling a DNA solution from a later stage of denaturation. This is not the hysteresis as defined above, but is another type of irreversibility originating in the strand scission with increasing temperature, which results in a complete dissociation of unfolded fragments.

The hysteresis depends strongly upon the ionic strength and the temperature of the solution,[8,51,154] because the potential barrier to the formation of a nucleus is formed by the electrostatic repulsion between two nucleotide chains to be folded. In fact, the hysteresis disappears at about one tenth molar salt concentration or higher.[29,96] It also depends upon the rate decrease of temperature.[51] The hysteresis appearing in some

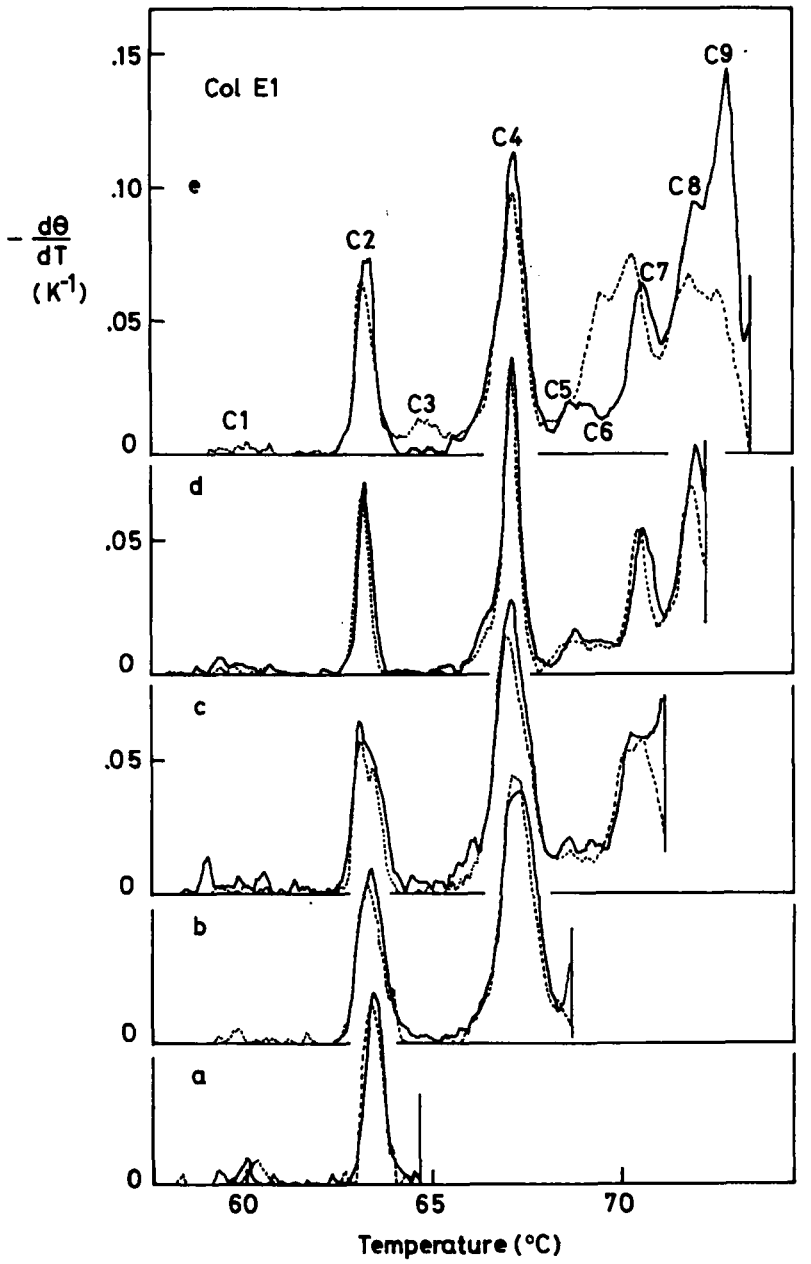

FIGURE 7. Differential profiles of melting (———) and refolding (------) of Col El DNA in 0.1 × SSC.[96] Profiles obtained with different turnback temperatures, T_r, are shown. Hysteresis appears T_r = 72.5 ~ 74°C. Rate of temperature change: 0.2°C/min.

melting steps disappears by the reduction of the rate of temperature change.[51] The fact indicates that there are several degrees of irreversibility in intramolecular nucleation.

As a typical example of the unfolding and refolding profiles of the DNA, which manifests a set of distinctive melting peaks, plots for plasmid DNA Col El are shown in Figure 7.[96] The figures represent several refolding processes which have started to cool from early stages of melting, together with the melting profiles to those stages. It is clear from these melting-refolding plots that the process is reversible up to 73°C; no hysteresis is observed until the peak C9 has been melted. According to the mecha-

nism of the hysteresis, this evidence indicates that none of the cooperatively melting (and refolding) regions which correspond to the peaks from C1 to C8 forms a local maximum of thermal stability. The hysteresis appears after the peak 9C and extends to the peak 5C at about 5°C below it.

Since the hysteresis originates in the sequence of cooperatively melting regions and their stability, it gives a clue for the location of these regions in the DNA.[51,52,157] Michel[51] studied this phenomenon for the purpose of developing a useful tool for mapping and has presented a detailed discussion of the principle and the technical procedures for the analysis. For higher molecular weight DNAs, however, it is hard to obtain a full picture of the arrangement of regions by a single procedure. A detailed examination of the DNA segments which have been fragmented by a controlled degradation with restriction endonuclease is of help for obtaining a complete map of the regions. New information about missing links in the sequence can be gained from the effect of a newly introduced chain terminus by enzymes.[51]

The rate of temperature change, which affects the extent of the hysteresis, may be another useful variable whose change will give new information on the arrangement of the regions.[51] Michel did pioneering work in the application of this method in the analysis and mapping of mitochondrial DNA of Yeast ϱ^+ and several strains of mutants ϱ^- (petite).[51] Regional maps were made for the DNAs of λ plac,[52,70] of plasmid Col El and its deletion mutant pN T1 (49.6% of Col El plus 6.6% non-Col El DNA inserted),[96,159] of mitochondria from rat liver,[87,160] and of SV40.[161] Furthermore, a combination of the method with electron microscopic observation has proved to be extremely powerful in constructing melting maps of high temperature resolution.[89,92,160,162]

VI. MODEL AND THEORETICAL CONSIDERATION

A. Molecular Factors Affecting the DNA Melting

The essential feature of the helix-coil transition, i.e., the melting of a DNA with N base pairs, is presented by a vector $\vec{S} = [S_1, S_2 \cdots S_N]$ in which an element S_i expresses the configurational state of the i-th constituent base of the DNA in a simplified manner; for instance $S_i = 1$ for a helical and $S_i = 0$ for a coil state. As far as the optical melting experiment is concerned, such a two-state model may be appropriate to correlate theory with experimental results, because only stacked bases ($S_i = 1$) contribute to the hypochromicity, which is linearly proportional to the degree of the stacking of bases.[11,12] On the other hand, the molecular factors affecting the vector $\vec{S}$ are the sequence of bases which is expressed by another vector $\vec{B} = [B_1, B_2 \cdots B_N]$ where B_i denotes the bases, A, T, G, or C, at i-th residue, and thermodynamic parameters characterized by the base species and the internal coordinates of the repeating constituents, the nucleotides. Both the enthalpic and entropic factor are involved in the thermodynamical factors, several of which are attributed to the nucleotide and its interaction with nearest-neighbor residues. They are the enthalpies of hydrogen bonding between complementary bases, of stacking between vertically neighboring bases, of the electrostatic interaction between charged phosphate groups, and of the entropy which comes from internal freedoms of the residue. The first and second factors favor the helix formation, while the third and fourth work against it; melting occurs as a result of the competition among these factors.

A complex feature is brought into the melting problem by long-range interactions which cannot be attributed to each nucleotide residue, that is, the electrostatic interaction under the low-ionic-shielding condition and the entropy factor arising from an internal loop. Therefore, the derivation of the temperature dependence of the vector $\vec{S}$ is not carried out directly in terms of the vector $\vec{B}$.

In order to examine the general characteristics of the melting phenomenon, let us consider first the case of homopolynucleotide, for which $B_i = B$ for each i. Such a molecular chain is treated within the category of the one-dimensional Ising model. Takahashi[163] first proved that different macroscopic phases cannot coexist in a one-dimensional system, where constituent elements have a single degree of freedom and nearest-neighbor interactions only. It was also proved in a general case where the elements have a limited degree of freedom and a finite range of interactions.[164] Mathematically, the result is expressed that the partition function of such system is given by the maximum eigen value of the transfer matrix, but the maximum eigen value is never degenerate in a finite matrix. Its physical meaning is that the energy of the boundary tension between phases, which provides a macroscopic phase, will never exceed the entropy of the mixing phases, which subdivide the phase into microscopic sections. This is because in a one-dimensional system, the coordination number is always 2, irrespective of the size of the phase boundary.[165] It has been shown, however, that if the interaction range is extended to infinity, the phase transition occurs even in a one-dimensional system.[166] This may be realized in the case of the DNA of infinite length, because the loop entropy mediates such infinite range interaction.[167] The amount of loop entropy is evaluated by considering the probability of the loop formation of two random coils of j residues which are joined end to end, that is

$$W = (j + 1)^{-c} \tag{4}$$

where $c = 1.5$ in the case of the three-dimensional Gaussian chain and 1.75, when the excluded volume effect is taken into consideration.[168] Thus the loop entropy attributed to the one residue in a loop of j residues is

$$S_{loop} = \frac{1}{j} kT \ln W = \frac{kTc}{j} \ln (j + 1) \tag{5}$$

where k = the Boltzman constant. Poland and Scheraga[3,169,170] examined the marginal condition for the phase transition and demonstrated that the constant c must attain certain values for the existence of a phase transition. According to their discussion in the case of a perfect matching model, the first-order phase transition occurs under the condition $c > 2$, and higher-order ones under $1 < c < 2$. In practice, in spite of their finite chain length, homopolynucleotides often manifest highly skewed transition peaks such that $\sigma_L >> \sigma_R \simeq 0$.[171] This fact indicates the significant contribution of the loop-entropy and chain-separation effects to the line shape of the transition. As a matter of fact, in the case of heteropolymers, natural DNAs, melting peaks in the higher-temperature region are usually sharper than those in the low-temperature region. Crothers[172] has explained the difference by stating that the low-temperature peaks correspond to the formation of local internal loops, whereas the high-temperature ones correspond to the unfolding of a GC-rich segment which is sandwiched by two unfolded regions. Therefore, the effect of loop entropy in the melting process is much larger in the former case than the latter, where the unfolded segment just adds a small fraction of unfolded chains to the large loop which has already been formed.

The effect of chain separation is another factor to be taken into account as well as the loop formation in the melting of the double helix.[173] The effect makes the peak of the highest melting temperature sharp. Therefore, the melting profile is, in principle, dependent upon the concentration of DNA chains. Quantitatively, however, the effect is negligibly small and should be practically unobservable in native DNAs.[173] In the special case of an all-or-nothing transition, which is realizable in oligonucleotide, the concentration dependency of the melting temperature is

$$\frac{1}{Tm_1} = \frac{1}{Tm_2} + \frac{R}{N \cdot \Delta H} \ln \frac{C_1}{C_2} \tag{6}$$

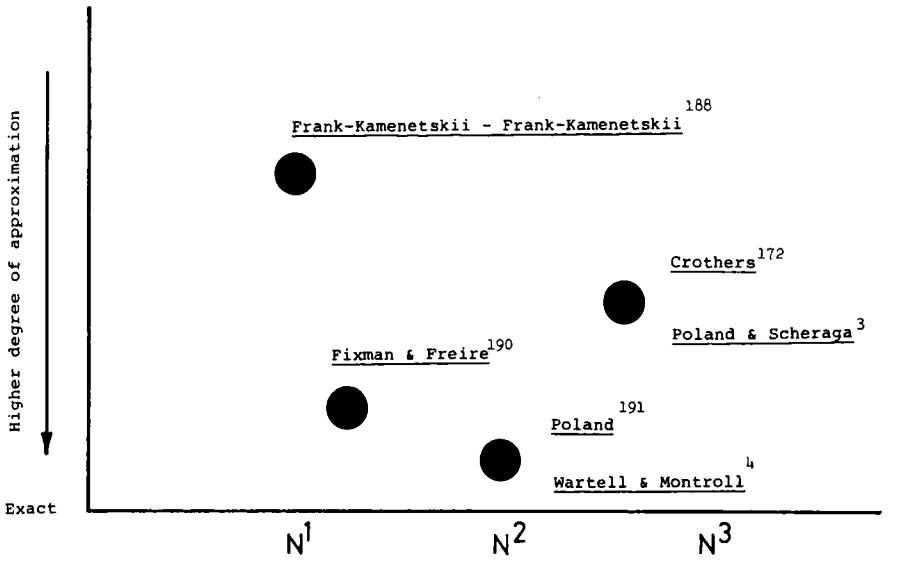

FIGURE 8. A Scatter plot indicating the characteristics of algorithms developed by several groups. The degree of approximation in the ordinate shows just a rough estimate on an arbitrary scale.

where T_{m1} and T_{m2} are the melting temperatures of the solute at the concentrations of C_1 and C_2, and $N \cdot \Delta H$ is the heat of association of nucleotide chains.[174] It is clear from the above equation that the concentration dependency is not a significant factor except for the case of small oligomers.

The essential feature in the melting of the natural DNA of a unique base sequence is that the local variation in the stability of the double helix competes with a tendency toward the formation of the macroscopic phase by the long-range interaction mentioned above. Earlier theoretical studies avoided this combined difficulty of long-range correlation and specific sequences either by taking an average of base sequence,[175-178] e.g., as a mixture of random copolymers, or by neglecting the effect of loop entropy.[179-184] Neglect of loop entropy is still an unavoidable step when one builds up an analytical formalism.[185,186] For periodic copolymers both the sequence and loop entropy are explicitly included in the calculation.[125,187]

B. Progress of Theoretical Studies

The theoretical study on the melting of sequence-determined DNA began in the middle 1960s, and has now established an algorithm for the calculation of the melting profile within the theoretical framework of the equilibrium thermodynamics of the perfect matching model with loops but without the electrostatic force. In Figure 8 the current status of several theoretical works is plotted in terms of the degree of approximation and of the number of steps in the numerical computation. The interrelation among the theories is exhibited in the form of a family tree in Figure 9. The complexity in the computational procedure may be explained in terms of the size of the matrix which generates the partition function. The size of the matrix, which indicates the extent of the incorporation of the long-range correlation and is 2×2 for the case where nearest-neighbor interactions only are considered, expands to $N \times N$ for the N-mer chain, if the loop entropy and other long-range interactions are involved. The number of the numerical operations, ν, in this case is proportional to the cube of N, $\nu \propto N^3$, so that it becomes practically impossible to carry out the calculation for chains with N >

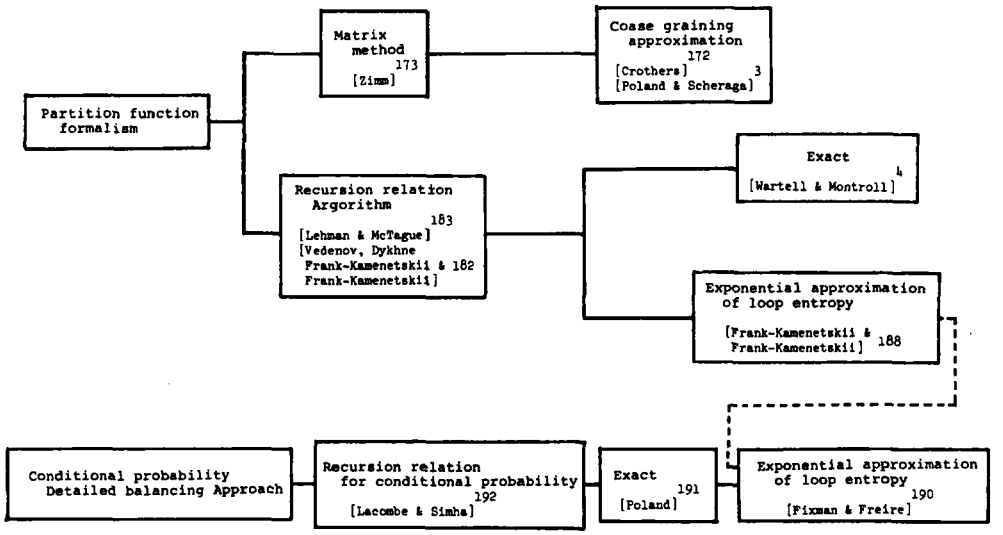

FIGURE 9. A family tree displaying the interrelation among the established equilibrium theories for the helix-coil transition of DNA where the base sequence and loop entropy are explicitly involved within the framework of the perfect matching model.

10^3. The coarse graining device proposed by Crothers and Kallenbach,[172,187] and Poland and Scheraga,[3] effectively and greatly reduces the matrix size from N × N to (N/M) × (N/M), where the segments of M residues long are considered to be the units constituting the molecule. Frank-Kamenetskii and Frank-Kamenetskii[188] succeeded in introducing the loop entropy effect into the recursion relation formula developed by Vedenov et al.[182] for which $\nu \propto N$. They approximated the loop entropy factor by an exponential function with undetermined variables

$$j^{-c} \simeq \mu g^{-j} \qquad (7)$$

where the variables μ and g are to be determined by iteration to obtain the partition function, which is consistent with the mean loop size $< j >$, to give a starting function $\mu g^{-<j>}$. The approximation was proved to be fairly good[189,190] (several percent error in the helix content) by comparing the result of the present method with that of Poland,[191] which has been accepted as an exact method.

Another line of development, besides formulating a partition function, was initiated by Lacombe and Simha,[192] who demonstrate that the conditional probabilities predicting the states of the unit having nearest-neighbor interactions are obtainable by recursion formulae which are the consequence of the detailed balancing relations of constituting units. Poland[191] extended this technique to the case of the DNA by incorporating long-range correlations. According to this technique the number of operations is $\nu \propto N^2$, so that sequences with thousands of bases can be treated exactly within the accuracy of current basic models. The Poland method has an advantage for obtaining microscopic quantities such as the state of the i-th residue; hence it is suitable for the depiction of the map of the stability distribution along the DNA. Another exact and independent method has been developed by Wartell and Montroll[4] who have succeeded in introducing the loop entropy effect into the theory of Lehman and McTague.[183]

Fixman and Freire[190] applied a clever technique of exponential-function approximation developed by Frank-Kamenetskii and Frank-Kamenetskii[188] to the loop entropy factor in Poland's formulation. Namely, by expressing the factor as the sum of several exponential functions

$$j^{-c} \simeq \sum_{i=1}^{I} a_i \exp(-b_i \cdot j) \quad (8)$$

the number of numerical operations can be reduced to I × N. With the use of appropriate values for the parameters, a's and b's, the error due to this approximation was found to be 0.4% ($j < 5000$) and 0.8% ($5000 < j < 7000$). Most of the recent theoretical calculations of DNA melting are based on this Poland-Fixman-Freire (PFF) method.

The PFF method has enough flexibility to adapt to changes in the model, for instance, to a different functional form of loop entropy, which is actually the case for a small loop where the stiffness of the chain may not be neglected. The advent of these exact techniques makes the theoretical calculation of DNA melting easily accessible for analytical purposes without having some misgivings about the computation procedure itself. In other words, coupled with the known base sequence of several DNAs and their high-resolution melting profiles, discussions can be narrowed down to one single issue, that is, the legitimacy of the model of the helix-coil transition of DNA.

The first problem of the long-range interaction in DNA melting by loop entropy has thus been overcome by the PFF method. The next obstacle to be overcome in the future is the electrostatic effect which spreads into both the folded and unfolded parts.

C. Computer Simulation of the Melting Fine Structure

By the PFF or the Poland method the melting fine structure of a DNA of a known sequence of $10^3 \sim 10^4$ bases long can be calculated. The agreement between measured and calculated results is fairly good, if suitable molecular thermodynamic parameters are selected. Figure 10 shows an example of the calculated results of the melting profiles of fd DNA and of one of its restriction fragments[62] by the Poland method with the base sequence determined by Schaller and Takanami.[193]

Before going into the examination of the nonregular base sequence we should first investigate the nature of the melting profile of periodic copolynucleotides which will give some fundamental idea about the extent of the cooperatively melting region and its appearance as a fine structure. Let us consider a periodic copolymer which has two blocks with lengths $l_b/2$ and base compositions $x_{GC} = (1-\Delta x)/2$ and $(1 + \Delta x)/2$, and are tandemly repeated. It can be shown that (1) long blocks melt independently of others at the temperatures characteristic of their own thermal stability; (2) as the block length becomes short, two peaks move closer to each other and finally coalesce into one peak; and (3) whether the coalescence of two peaks occurs or not is dependent upon the difference in the base compositions of two blocks (Δx), the block length (l_b), and the parameters characterizing the cooperativity (σ and c). The heterogeneity of the base sequence may be characterized by the first and second parameters, which are approximately proportional to $\Delta x \cdot l_b$.[49] The phase diagram which depicts the above-mentioned situation of melting peaks and block sequence is shown in Figure 11.

1. Melting Profiles of Randomly Generated Base Sequence

Computer simulation for the melting of a model polynucleotide, the base sequence of which has been randomly generated, indicates that (1) a fine structure appears for short chains less than 10^4 bases long ($\sigma = 10^{-4} \sim 10^{-5}$)[45,49,107,172] (2) a fine structure disappears when the chain is longer than 10^5 or the loop entropy is neglected;[45,181] and (3) without the loop entropy factor a fine structure appears in longer chains if cooperativity increases ($\sigma \sim 10^{-8}$).[45] These facts indicate that the statistical fluctuation in a finite random sequence produces distinct fine structures. As a matter of fact, the base sequences of the DNA of ϕX174 phage has been shown to be random according to several statistical criteria. For instance, the local segmental distributions of G + C content in the fragments of ϕX174 agree well with a binomial distribution curve,[80,108]

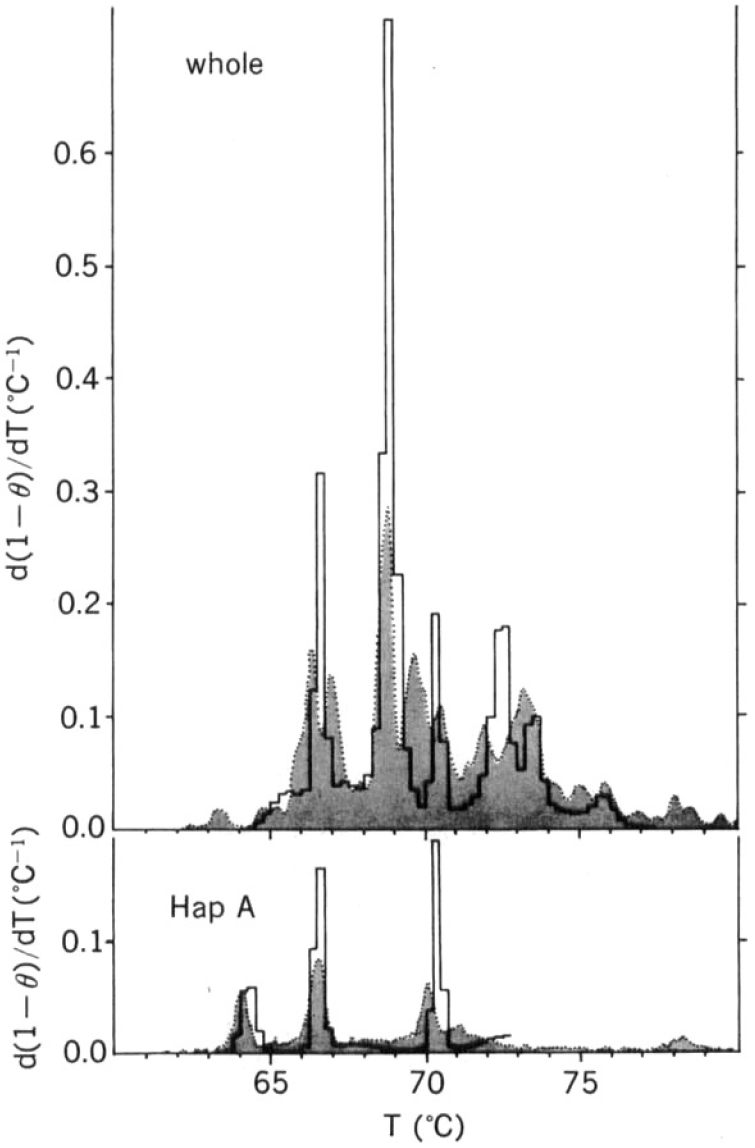

FIGURE 10. A comparison of theoretical (———) and experimental profiles (-------) of whole fd DNA and its HapA fragment.[62] The molecular parameters used in the calculation are listed in Table 3. Solution: 0.1 × SSC. (From Wada, A., Ueno, S., Tachibana, H., and Husimi, Y., *J. Biochem. (Tokyo)*, 85, 827, 1979. With permission.)

when the base composition is averaged over a relatively short stretch of the segment.* On the other hand a remarkable deviation from a smooth binomial distribution ap-

* One way to display the characteristic of a base sequence is the distribution function of $P_n(x)$ of the G + C content (x) of sections along the entire DNA, each containing n base pairs;[80] the first section for averaging the G + C content starts with the first base pair, the second with the second base pair, and so on until the whole fragment is covered. If the base sequence of the fragment is purely random and sufficiently long compared with the length of the section (n) the distribution function should agree with the binomial function.

$$P_n(x) = \frac{n!}{\{n(1-x)\}!\,\{nx\}!} X_0^{nx} (1 - X_0)^{n(1-x)}$$

where X_0 is the G + C content of the whole chain examined.

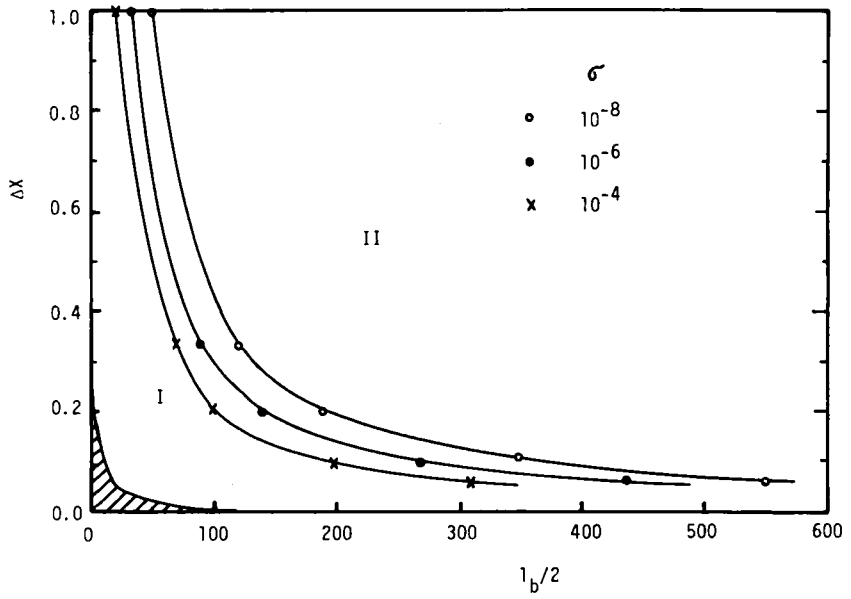

FIGURE 11. Heterogeneity-homogeneity (double peak-single peak) "phase diagram" was calculated for hypothetical periodic block copolynucleotides with several degrees of cooperativity. Abscissa: half period $l_b/2$. Ordinate: amplitude of (G + C) content Δx. For example, the polynucleotide $(AGAAGAGAGGAG)_{300}$ is expressed by $l_b/2 = 6$ and $\Delta x = 0.333$. The thermodynamic parameters used are the same as in Reference 108 (cf. Table 3) except for the cooperative parameter σ. In domain II, a biphasic transition occurs; that is, the length of the cooperatively melting region is equal to $l_b/2$ and the melting fine structure can be observed. In domain I, a monophasic transition occurs. The boundary curve is dependent upon the cooperative parameter σ, and expressed approximately by the equation $\Delta X \cdot l_b/2 \simeq -5 \log \sigma$.

pears when it is averaged over several hundred bases (Figure 12). The deviation may come from the fact that the segment length for the averaging 500 base pairs, is no longer negligibly short when compared to the whole length. At the same time, it is still possible to suspect that some nonrandom sequence exists as seen in fd DNA. In any case, it is dangerous to define the random sequence for a fragment of limited length.

An interesting fact exhibited in the distribution function of a long averaging length ($n \sim 500$) is that the profile is quite similar to the melting profile. It suggests that the length of the cooperatively melting region is about 500 base pairs long. This has actually been proved by the result of a computer simulation for the ϕX174 and fd DNAs.[62,78,80,108,194,195]

With the molecular thermodynamic parameters of DNA and by neglecting the heterogeneity in the stacking, the width of melting peaks becomes about 0.5°C. This is equivalent to that of the experimental result,[45] while the RNA parameters with stacking heterogeneity give a peak width of several degrees.[49]

D. Several Problems of Current Theoretical Studies

Current theoretical studies and DNA models used therein involve several simplifications and approximations, some of which have to be seriously examined. The premise of perfect matching of the two strands in the DNA in the melting-refolding equilibrium is feasible in the case of the natural DNA with a unique sequence. Extra structures, however, should be accounted for in the evaluation of the partition function in some special cases such as the staggered structure of hairpin loop formation at the d(A-T) repeat of crab satellite DNA or the palindrome sequence found in several

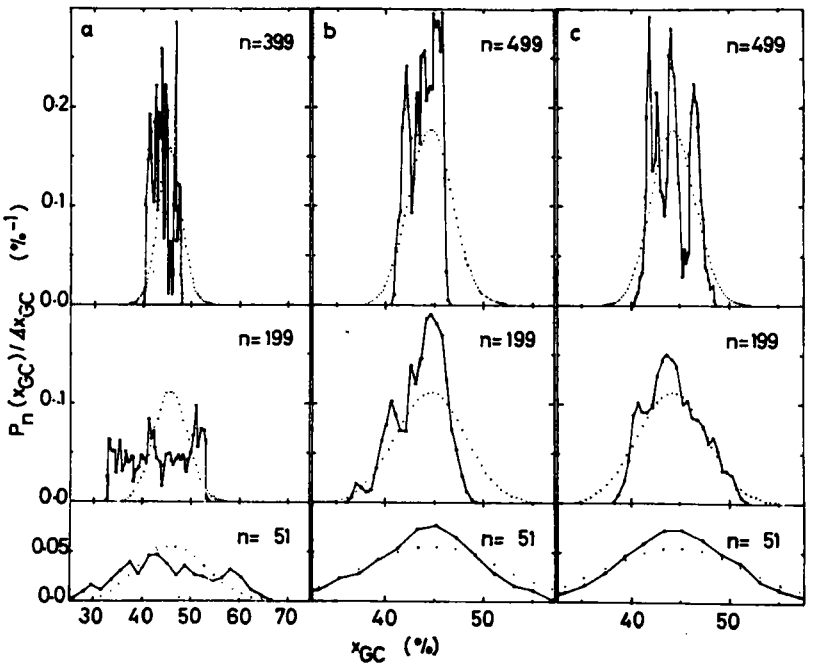

FIGURE 12. Local segmental distributions of G + C content in (a) HapC fragment of fd DNA, (b)Y2, and (c)Y1 fragments of ϕX174 DNA.[108] The distribution function, Pn (X), is expressed in terms of the G + C content, X, of sections each containing n base pairs along the DNA fragment (see text for the detail). For each fragment three distributions are plotted with different section size, n. The binomial distributions are also plotted in the same figure by dotted line. (From Ueno, S., Tachibana, H., Husimi, Y., and Wada, A., *J. Biochem. (Tokyo)*, 84, 917, 1978. With permission.)

DNAs. Even so, since the hairpin structure is still relatively unstable compared to the regular double helix, its effect on the melting profile may not be large.

The single cooperative parameter, σ, currently used includes base to base stacking energy as far as theoretical formalism is concerned. The stacking energy depends upon the kind of base pairs involved so that the value of the cooperative parameter should vary along the molecular chain. This kind of modification to give a sequence-dependent variation of σ can be carried out in Poland's theoretical framework.

A similar problem has brought about the necessity of incorporating the next-nearest-neighbor interaction into the calculation. As a matter of fact, oligo dA differs from oligo rA in that the base to base stacking in a single strand is absent in oligo dA; hypochromicity is smaller in the polymer than in the oligomer. Vournakis et al.[196] accounted for this evidence in terms of the anticooperativity due to the repulsive interaction between next-nearest neighbors in the DNA, while the hydrogen bonding by 2′-OH group compensates for the repulsive force in the RNA. The origin of the repulsive force has been considered to be charged phosphates which are separated by about 6 Å. The effect can be taken into the calculation in a relatively high salt condition as the next-nearest-neighbor interaction, when the Debye shielding radii are comparable to the distance between charges.

As for the base to base stacking energy, it may differ according to the ten different structures in stacking AT and GC base pairs in the DNA double helix. The differences can be easily incorporated into the rigorous algorithm for the melting calculation.[49,197] However, reliable data for ΔHs′and ΔSs′are lacking for each of the ten stacking structures. The stacking heterogeneity has been estimated to have an influence of about

0.2°C in T_m,[197] which is fairly small compared to the primary effect of G + C content. In principle, however, the Marmur-Doty relationship is deformed to some extent by the stacking heterogeneity.[183,198]

The existence of a polymorphous double helix has been suggested from several experimental results.[40,199,200] These results will also bring complex factors into both the model and the variation in parameters.

Electrostatic interaction with moderate ionic strength extends beyond several residues in the DNA (the Debye radii in 0.1 SSC solution is 20 Å). The PFF theory cannot include this effect explicitly into its algorithm. What is usually done is to incorporate the effect intrinsically into the parameters of the long-range interaction, such as σ, c, or β. Gotoh et al.[72] tried to incorporate the electrostatic interaction in the parameter σ. On the other hand, the calculation in which the electrostatic effect is included solely in the energy of local base pairing does not express the real situation.[79] The existence of a long-range interaction in a low ionic strength condition was experimentally demonstrated with block oligomers; namely, d $(C_{15} \cdot A_{15}) \cdot d(T_{15} \cdot G_{15})$ melts in the single mode (one peak) in 0.01 *M* NaCl, but in the double mode (two peaks) in 1 *M* NaCl.[132]

Is it adequate to examine the observed melting profile in terms of equilibrium thermodynamics? As the observed transition manifests a clear hysteresis under some experimental condition as described in Section V, the situation is not in thermal equilibrium. Therefore, theoretical discussion should be confined within the condition of nonhysteresis, that is, the melting of fairly short DNA fragment in relatively high ionic strength.

There is another fact which should be noted in comparing a calculated profile with a fine structure experimentally obtained. The base sequence which has been established by chemical analysis and is used in the calculation is not always unique; a sizable population of DNAs in the optical cuvette may have some different sequences. For instance, among the wild type Qβ-RNA, the amount of the molecules having a standard base sequence is only several percent of the total.[201] Furthermore, even in the ϕX174[202a] or fd DNAs[193] several percent of the whole base sequence is still uncertain. Vizard et al.[79] tried to find the effect of the uncertainty in base sequence on the melting profile by introducing a 3% random substitution of base pairs into the sequence of ϕX174 DNA. According to their report, no visible change in the profile resulted; hence the melting profile seemed to be rather insensitive to a small variation in the sequence. On the other hand, a contradictory result has also been obtained. A revised version of the base sequence of ϕX174 DNA was recently published[202b] which differs at 30 positions from the old one, and adds an additional sequence of 12 base pairs. The changes in these 42 bases (about 0.8% of the total number of bases) potentially affect the calculated melting profile. The melting profiles calculated with the old and new base sequences are compared in Figure 13. The relatively large difference found between them is due to the fact that the changes are not randomly distributed but rather clustered.

VII. MOLECULAR THERMODYNAMIC PARAMETERS CHARACTERIZING DNA MELTING

The thermodynamic parameters appearing in the theoretical formulation in the last section are (1) the enthalpy, ΔH_i, and entropy, ΔS_i, which are allocated to the i-th base pair which form a stacked structure at an end of helical section already formed; (2) the free energy which is given as $\Delta G_i = \Delta H_i - T\Delta S_i$; (3) cooperative parameter σ; (4) the loop entropy exponent c; and (5) the chain association parameter β_e. When the base sequence is explicitly considered, ten different stacking modes should be separately taken into account by the use of suffix i, which runs as $\overrightarrow{AT}$, $\overrightarrow{TA}$, $\overrightarrow{AA}$, $\overrightarrow{GC}$, $\overrightarrow{CG}$,

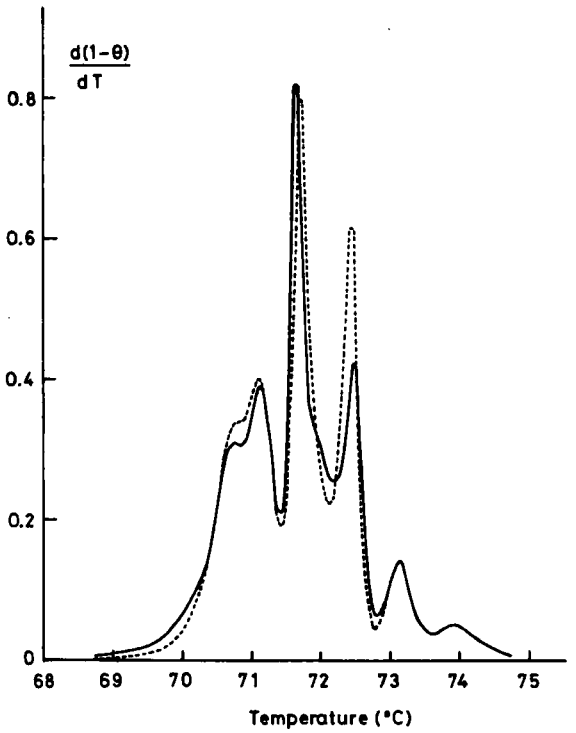

FIGURE 13. Theoretical melting profiles of whole DNA of ϕX174. Solid line is for the new base sequence and dotted line for the old one. Thermodynamic parameters are the same as the ones used in Reference 108, except $\sigma = 5 \times 10^{-5}$.

$\vec{G}\vec{G}$, $\vec{A}\vec{G}$, $\vec{A}\vec{C}$, $\vec{T}\vec{G}$, and $\vec{T}\vec{C}$, where $\vec{A}$, $\vec{G}$, $\vec{T}$, and $\vec{C}$ indicate the base pairs of AT, GC, TA, and CG, respectively. Usually, by considering the Marmur-Doty relationship which is empirically valid, the number of parameters is reduced as follows:

$$\Delta H_{\vec{A}\vec{A}} = \Delta H_{\vec{A}\vec{T}} = \Delta H_{\vec{T}\vec{A}} = \Delta H_{AT} \quad (9a)$$

$$\Delta H_{\vec{G}\vec{G}} = \Delta H_{\vec{G}\vec{C}} = \Delta H_{\vec{C}\vec{G}} = \Delta H_{GC} \quad (9b)$$

and

$$\Delta H_{\vec{A}\vec{G}} = \Delta H_{\vec{A}\vec{C}} = \Delta H_{\vec{T}\vec{G}} = \Delta H_{\vec{T}\vec{C}} = \frac{1}{2}(\Delta H_{AT} + \Delta H_{GC}) \quad (9c)$$

The same is true for the entropy parameters. Sometimes T_m is used instead of the entropy parameter, namely ΔS_{AT} (or ΔS_{GC}), or is substituted by $\Delta H_{AT}/T_{m,AT}$ (or $\Delta H_{GC}/T_{m,GC}$) with some correction factors for loop formation.

A. Evaluation of Parameters for Synthetic Poly- and Oligo-Nucleotides

A number of synthetic homo-polynucleotides and the co-polynucleotides which have a repeating sequence have been studied. Their T_m's and ionic strength dependency are reviewed by Wells et al.[40]

The transition width of these homogeneous polydeoxynucleotides is about 0.5°C[48,126,133] and is almost independent of the ionic strength of solutions,[126,133] or it is slightly changed from 0.60 to 0.40°C by the change in the Na^+ concentration from 45 to 3 m*M*.[203]

Wells et al.[120] investigated the T_m of several synthetic copolynucleotides having different stacking modes and found the following differences:

Structure A $\begin{pmatrix} AA \\ TT \end{pmatrix} - \begin{pmatrix} AT \\ TA \end{pmatrix} : + 7°C$ Structure B $\begin{pmatrix} GG \\ CC \end{pmatrix} - \begin{pmatrix} GC \\ CG \end{pmatrix} : - 12°C$

Structure C $\begin{pmatrix} TC \\ AG \end{pmatrix} - \begin{pmatrix} TG \\ AC \end{pmatrix} : - 6°C$ Structure D $\begin{pmatrix} TTG \\ AAC \end{pmatrix} - \begin{pmatrix} TTC \\ AAG \end{pmatrix} : + 3.5°C$

This evidence indicates that the Marmur-Doty relationship is no more than a first approximation.

At the present, however, it is not clear whether the deviation from its linear relationship originates in the heterogeneity due to the ten different stacking modes, or in the polymorphism of the double helical structure other than the B form. The fact that common parameters could not be consistently determined from the T_m's of these copolymers suggests the existence of polymorphysim.[197] On the other hand, in the case of RNA, the stacking heterogeneity was observed and parameters were determined by a series of melting measurements.[204] In any case, more quantitative experimental data are required to determine enthalpy and entropy parameters for the ten stacking modes.

The same situation has been found in the study of synthetic oligomers having specific sequences.[23,128,130,132,205-207] The meltings of three different block oligonucleotides cannot be reproduced by a set of common parameters.[132]

B. Natural DNA

Average values of the thermodynamic parameters, $\overline{\Delta H}$ and $\overline{\Delta S}$, of natural DNA were obtained by calorimetric measurements.[208] ΔH was found to depend upon G + C content; the extrapolation of the measured values to pure AT and GC polymers gives $\overline{\Delta H}_{AT}$ = 7.2 kcal/mol and ΔH_{GC} = 9.0 kcal/mol.[208] The ionic strength dependence of $\overline{\Delta H}$ is about 0.5 kcal/mol over a tenfold change in the Na^+ concentration,[209,210] while $\overline{\Delta S}$ is much less dependent upon either G + C content or ionic strength than $\overline{\Delta H}$.[209-211] This is quite a contrast to the case of RNA in which the higher stability of the GC pair as opposed to that of the AU pair is mainly due to an entropic factor.[212]

Since 1977 base sequences of fairly long DNAs have been determined, which allowed us to perform a detailed examination of the parameters in the light of empirical evidence. The parameter values may, in principle, be determined so as to give the best fitting curve to an experimental one. However, the fine structure profile is often insensitive to the value or values of some parameters. For instance, in the case of DNA fragments Y1 and Y2 from ϕX174, the shapes of their melting fine structure are left unaltered by changing ΔH_{AT} between 5.6 and 8.6 kcal/mol and ΔH_{GC}-ΔH_{AT} between 0.3 and 3.0 kcal/mol.[106] The reproduction of the experimental profile by computer simulation is qualitatively adequate,[62,106,108,194] but is not good quantitatively in general (see Figure 10). The disagreement seems to be due to a defect of the molecular model itself rather than a wrong choice of parameters. Especially at low ionic strengths below 10 m*M* [Na^+], the reproduction seems very poor.[106] In Table 3 are listed the parameters which have been used by several research groups to reproduce the melting profile. The simulated curve using these parameters gives a fine structure where each peak has a line width of about 0.3 $\sim$ 0.6°C, while empirically it is about 0.5°C as mentioned

Table 3
MOLECULAR THERMODYNAMIC PARAMETERS USED FOR THE REPRODUCTION OF EMPIRICALLY OBTAINED MELTING PROFILES OF SEVERAL SEQUENCE-DETERMINED DNAs BY COMPUTER SIMULATION

DNA	Ionic condition	Experimental method[a]	$-\Delta H_{AT}$	$-\Delta H_{GC}$	$-\delta_{AT}$	$-\Delta S_{GC}$	Tm_{AT}	Tm_{GC}	σ	C	β [M^{-6}]	Ref.
			kcal/mol			e.u.						
ϕ174 RFII	0.1 × SSC	A	8.0	9.04[b]	24.6[b]	24.6[b]	52.5	94.9	5×10^{-5}	1.5		78,235
ϕX174 RFIII	30 m*M* [Na^+]	A	8.0	9.03[b]	24.3[b]	24.3[b]	55.7	98.1	5×10^{-5}	1.5		79
	195 m*M* [Na^+]	A	8.0	8.99[b]	23.4[b]	23.4[b]	68.2	110.6	5×10^{-5}	1.5		79
ϕX174 Y_1	0.1 × SSC	A	6.6	7.6	20.3[b]	20.6[b]	51.5	96.5	1.6×10^{-4}	1.75	670	108
ϕX174 Y_2	0.1 × SSC	A	6.6	7.6	20.3[b]	20.6[b]	51.5	96.5	2×10^{-6}	1.75	63	108
fd HapC	0.1 × SSC	A	6.6	7.6	20.3[b]	21.3[b]	51.5	96.5	5×10^{-9}	1.75	1.4	108
	0.1 × SSC	A	7.6	7.9	23.3[b]	21.3[b]	53.0	97.7	7.4×10^{-9}	1.75	90	106
fd HapCHael	0.1 × SSC	A	7.6	7.9	23.3[b]	21.3[b]	53.0	97.7	7.4×10^{-9}	1.75		106
ϕX174 Y_1, Y_2	0.1 × SSC	A	8.0	9.24[b]	24.8[b]	24.8[b]	49.7	99.9	3.5×10^{-8}	0		185
$(dA)_n + (dT)_n$	14 m*M* [Na^+]	A	8.02	—	24.8	—	50.54		4.5×10^{-5}	1.55		125
$2(dA\ dT)_n$	14 m*M* [Na^+]	A	7.87	—	24.8	—	44.30		6.8×10^{-5}	1.55		125
$(dAAT)_n + (dATT)_n$	14 m*M* [Na^+]	A	7.92	—	24.8	—	46.30		4.5×10^{-5} 6.8×10^{-5}	1.55		125
$2(dA\ dT)_n$	5m*M* [Na^+]	C	7.9 ± 0.14	—	24.8[b]	—	40					236
2(ATGCAT)	40 ~ 50 m*M* [Na^+]	N	4.7[c]	—	15.2[c]	—	40[c]					205
Cl. perfringens *M. lysodektious*	1 m*M* [K^+] +0.01 SSC	C & A	7.2	9.0	23.2[b]	24.4[b]	37[d]	95[d]				208
Salmon sperm fd	0.1 × SSC	A	8.0	9.04[b]	24.6_{2b}	24.6[b]	52.5	94.9	5×10^{-5}	1.5		194
$2(GC)_i$ $i = 4 \sim 7$	1.1 *M* [Na^+]	A	—	11.1	—	27.9	—	124		—	1.6×10^{-4}	23
$(C_iA_i) + (T_iG_i)$ $i = 15,20$	10 m*M* [Na^+]	A	*8.41[b] 8.51[b]	9.15[b]	24.8	24.8	*66 70	95.6		—	0.1	132
$j = 10,15$	10 m*M* [Na^+]	A	*8.01[b] 8.11[b]	8.75[b]	24.8	24.8	*50 54	79.5		—	0.01	132

[a] A, absorbance; C, calorimetric; and N, NMR measurement.
[b] Calculated from a relationship $\Delta H = T_m \Delta S$.
[c] Terminal base pair.
[d] Extrapolated from experimental data.
* Showing stacking heterogeneity.

earlier. The average length, n residues, of the segment which melts by an all-or-none mode is related to the line width by

$$\Delta T \simeq \frac{4R\ T_m^2}{n \cdot \Delta H} \qquad (10)$$

where R is the gas constant.[213] The width of 0.3°C corresponds to cooperative melting over 400 base pairs. On the other hand, long-range fluctuations in base composition over 200 to 1000 base pairs have been found in the DNA of ϕX174 and fd, where melting occurs in accordance with this compositional block.[62,106,194,195] Namely, the primary factor determining the cooperatively melting region is the fluctuation in the G + C content.

VIII. PROBING INTO LOCAL VARIETIES OF DNA DOUBLE HELIX

In the preceding sections, the fine structure in the melting of the DNA was correlated with a discrete unfolding process from one cooperatively melting region to another. The physical origin of the occurrence of these regions was described in terms of the base sequence of the DNA. This correlation between physical and chemical sequences is, however, not derived straightforwardly; in other words, the melting map is not evident at first glance of the running average of the local G + C content (Figure 14). This is because, as described in Sections V and VI, the long-range effect due to the cooperative nature of the stability of the DNA double strand makes the relation ambiguous. Several factors such as (1) a specific fluctuation in the base sequence over a fairly long stretch of the DNA strand, (2) a localized highly stable region consisting of GC pair clusters which plays the role of the stopper of unfolding, and (3) loop formation in unfolded regions, determine in a subtle way the division of the cooperatively melting regions in the DNA.[45,49,52,108,194] In the present situation where a complete physical and quantitative understanding has not yet been attained, we may not expect too much from the high temperature-resolution study alone as a tool for probing the helix stability distribution in connection with the base sequence or genetic structure of DNA. Even so, the unique and abundant information obtainable by the melting study has now been found useful in various aspects of DNA research, some of which will be presented in the following sections.

A. Nature of the DNA Base Sequence

The statistical nature of the base distribution has so far been examined for many DNAs by several different analytical methods. The most direct measurement among them is, of course, that on the DNA of ϕX174 and fd phages, the whole base sequences of which were recently determined.[193,202] As far as the short-range arrangement of bases which are examined by criteria such as the nearest-neighbor base frequency, the autocorrelation function, and the binomial distribution function (see the footnote in Section VI) is concerned, the base sequences of ϕX174 DNA is found to be random;[106] it is the quasi-random sequence according to the terminology of the Russian school.[5,37,45,107] For fairly long DNAs of bacterial and higher organisms, in spite of a large variation in their average G + C contents ranging from 25 to 75%, the distribution of the base composition in individual DNAs was found not to deviate much from random ones when it is observed in CsCl density-gradient experiments.[214,215] Sueoka[216] and Freese[217] interpreted this evidence as due to a species-specific balance in the equilibrium of the GC ⇌ AT transversion. It seems to be a characteristic of DNA to have a quasi-random base distribution which provides a rather narrow spread of the base

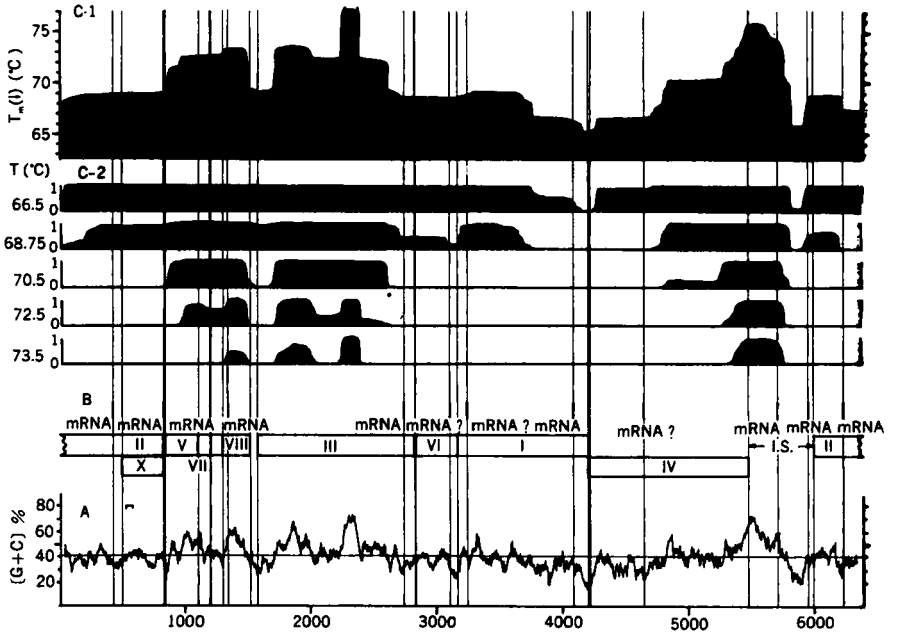

FIGURE 14. Three kinds of maps characterizing fd DNA:[62] (A) distribution of G + C content, (B) genetic map, (C) stability map calculated from the base sequence, (C-1) helix probabilities at successive temperature points, (C-2) stability of the double helix indicated by the local melting temperature defined as the temperature giving a probability of 50% helix to each of the bases. (From Wada, A., Ueno, S., Tachibana, H., and Husimi, Y., *J. Biochem. (Tokyo)*, 85, 827, 1979. With permission.)

composition around its characteristic mean value.* Several other interpretations of this tendency in the DNA were also published.[109,218-220] All of them have explained it as a result of evolutional processes, where the quasi-random base distribution is suitable for the biological functions.

It was found, however, in several short viral DNAs that their base sequences highly fluctuate and manifest a blockwise feature.[32,109,221] The same thing was found to be true in the case of several bacterial DNAs.[110,222] Since many of the organisms having this type of DNA are those being associated with the recombination or transduction phenomena, for instance temperate phages and plasmid DNAs, the block sequence seems to be a product of the exchange of local segments between two homogeneous DNAs of quasi-random sequences with different average base compositions.[109,110] The block sequence may alternatively be explained, if Sueoka-Freeses base homogenizing mechanism works within one DNA with regionally different equilibrium constants of the transversion. In any case the melting profile reflects these characteristics of the DNA base sequence much more precisely than any other methods. Although the quasi-random sequence itself produces more than one peak within a narrow temperature interval, the block sequence manifests, as a heterogeneous mixture of these profiles, many more peaks over a fairly wide temperature range.

* If the GC and AT base pairs are randomly sampled from a population where the G + C content is fixed at some given value (X_o) a random sequence will result, while the histogram of the local G + C content (x) of the sequence of length n will be a fairly narrow binomial function whose center is at X_o as explained in Figure 12. The problem here is why individual DNAs belonging to different species tend to have their own unique X_o values. The term "quasi-random sequence" means a single X_o value for the whole DNA chain. The "block sequence" means a sequence with several different X_o values.

B. Any Relation to Genetic Unit?

Since the minimum size of the cooperatively melting region is on the order of a hundred base pairs, a single genetic unit may contain several of them.[62,108,195] Yabuki, Gotoh, and co-workers[49,53] found that several melting peaks in the melting profile of the DNA of a wild type of bacteriophage λ disappeared in the DNA of deletion mutants. This by no means shows that the genetic unit corresponds to some definite melting peaks, but the deletion is shown to be clearly detectable by the melting study.[37,49,53] Tong and Battersby[195] noticed an interesting fact in the melting map of ϕX174 DNA; that is, if the DNA is divided into segments marked by the locations where sudden changes occur in the melting map and if the G + C contents are calculated for each of these segments, a marked correlation appears between the local G + C content and the melting region. On the other hand, the distribution of the G + C content of individual gene sections does not seem to show any significant feature along the DNA strand. This indicates that there is no apparent correlation between the cooperatively melting regions and genes.

There are, however, many meaningful coincidences which are found between the boundaries of the cooperatively melting regions and those of the genes in the DNAs of ϕX174,[108,195] fd,[62] SV40,[195] and λ plac DNA;[52] a typical case is shown in Figure 14. It was also pointed out by comparing the melting map and the genetic map of ϕX174, that the ends of genes, including those of overlapping genes, are regions which melt at low temperature, but that the converse is not true.[195] As a matter of fact, much evidence has been found to show that the DNA segments interspersed in the structural genes are AT rich.[103,223] Furthermore, more evidence suggesting a correlation between the local base composition and biological function is that the left half of λ DNA, which produces a broad melting band in the highest temperature region, is considered to perform structural coding, while the multiple peaked region at low temperature corresponds to the melting of the right half which carries a set of information on genetic functions such as the replication of DNA and the recombination.[25,52,160] It is interesting to note that the right half of λ DNA has a much higher density of digestive sites of restriction endonucleases than the left half.

Now, in the discussion on the correlation between the melting and the genetic map one might suspect that the cooperatively melting region is just an exceptional and accidental feature of the DNA in vitro under special conditions of high temperature and ionic strength, and that it would be nonsense to consider its biological role seriously. This is not quite true, because the melting map is a map that indicates the distribution of local stability which makes sense in the case of the transient opening[37,224] (the breathing) of the DNA double helix, in the local conformation transition among different double helical structures,[200,225,226] and in the action of DNA unwinding proteins which unfold the double helix at room temperature.[224,227] One may also speculate that each of the regions having unique stabilities is a domain within which the telestability effect is confined. Namely, the range of the transmission of the allosteric effect through DNA double strand (the term coined by Hogan, Dattagupta, and Crothers[237]) gives indirect influence by one bound protein or ligand molecule on the binding of another at a distance due to a structural alteration of the DNA segment that intervenes between these two sites. It may be limited to within a domain formed by a cooperatively melting region. The authors are tempted to conjecture that the melting fine structure is just a high-temperature manifestation of domains of different stability which are actually working for the telestability regulatory effect at room temperature. As a matter of fact, the location of the boundaries of the cooperatively melting regions are found to be well conserved over a wide range of ionic concentrations (see Figure 3 and 4).[72,118,119] The computer simulation indicates that they also remain relatively unchanged against the change of the thermodynamic parameters of the helix-coil transition.[62,106,108] These

regions are, therefore, intrinsic to DNA molecules and their specific sequence. Besides these empirical indications quite a few people suspect that the cooperatively melting characteristic and regions should have some more important biological meanings, because living organisms have always utilized any, even slightly, advantageous characteristics found their constituent materials, and have incorporated them into genetic sentences as hereditary information during the course of evolution. The redundancy in genetic code due to the wobbling of the third base of the codon would provide a possible margin to adjust the local G + C content by the use of synonymous codons.

C. As a Tool for the Functional Analysis

1. Comparative Study of the Homology and Taxonomy of DNAs

The melting profile manifests the nature of the base sequence in the form of a histogram of the local G + C content arranged over several hundred base pairs. It provides, therefore, a convenient method to examine the homology or to explore the taxonomic relations among DNAs. The distribution of base composition can also be observed by density-gradient centrifugation and electron microscopy. The resolution of the first method, however, depends upon the length of DNA fragments for which the dispersity of the buoyant density is measured.[228] In usual cases the minimal length of the fragment is an order of 1000 base pairs, so that the buoyant density distribution has a lower resolution than the local Tm distribution which has a resolution of about one hundred bases.[85] On the other hand, the electron microscopic observation of the intermediate melting states of the DNA is an extremely powerful method to locate the unfolded locus in the DNA strand.[229,230] Its application, unfortunately, is restricted to relatively short DNAs. Also, formamide or formaldehyde, usually used for maintaining an intermediate state of the DNA, depresses the cooperativity in the stability of the double helix. Therefore, the melting map exhibits the local G + C composition with a very short average window and the information on the cooperatively melting region is lost. Therefore, these observing techniques may be used in such a way that they complement one another. Homology among the viral DNAs of T_3, T_7, and BF 23 was discussed by comparing the apparent resemblance of their melting profiles.[74]

In the study of DNAs of wild type λ phage and its mutants, the partial deficiency of a segment in the deletion mutants was found to appear clearly as the absence or shift of several melting peaks.[49,53] The base composition of the deleted sites estimated by the melting profile agrees well with the result with ultracentrifuge analysis; furthermore, it shows more structure than that obtained by the ultracentrifuge analysis. A comparative study on plasmid DNA Col El and its mutant pNTl, which consists of 56.2% Col El DNA and involves an inserted non-Col El sequence of about 6.6%, demonstrated that the melting curve of Col El consists of three groups: those located in the region common to both DNA, those in the deletion region, and those from the inserted region.[96]

A series of well-organized and systematic studies on the mitochondrial DNA and its ϱ^- mutants was carried out by the French school.[90-93] An interesting feature in the ϱ^- mutants is their variety in the complexity of DNAs in which different parts of the wild type mitochondrial DNA are repeated and amplified in various combinations up to a hundred with practically no common sequence. Therefore, the purified sequence offers an amplified version of a given segment of the mitochondrial DNA suitable for the melting analysis. A point particularly noteworthy in their study is the well-balanced and -combined use of a variety of melting techniques; namely, the high-resolution melting measurement, the refolding technique already mentioned in the preceeding sections, the kinetic method, the so-called Cot analysis, and the electron microscopic study together with the genetic analyses. The complexity and polydispersity of the melt-

ing profile were found to be well reflective of the sequence and genetic complexity of the mutants measured by the renaturation kinetic method. Furthermore, the study was extended to show that particular peaks in several mutants are those associated with the difference in genetic recombination.[91-93]

In a combined study of melting-refolding profiles with high-resolution and electron microscopy on the rat liver mitochondrial DNA, Yonekawa et al.[160] found that the DNA has five early melting AT-rich regions, all of which are located in one half of the molecule. They also found that the melting maps are remarkably similar for mitochondrial DNAs, several plasmid DNAs, and phage DNAs, all of which have several AT-rich regions which are clustered together in one half of the DNA molecule. Since in many of these DNAs, the AT-rich regions have been found to play an important role in the genetic recombination, integration, and excision functions, they suspect that the AT-rich region may carry a function for the interaction with another DNA.

Steinert and Van Assel[105] carried out a high-resolution melting analysis on the kinetoplast DNAs isolated from four species of hemoflagellates. They found that each of the melting profiles is highly heterogeneous and specific to the species, which indicates that the base sequence varies even between apparently closely related ones. They have presented an interesting problem for the evolutionary process of kinetoplast in that the high rate of change of the base sequence of DNAs observed is in sharp contrast to the conservative structure of kinetoplast itself, which has been maintained with very little structural alteration during the evolution.

Guttman, Vitek, and Pivec[85] compared the melting profiles among twelve mammalian liver nuclear DNAs. Most of the fine structures in this case come from the intermolecular heterogeneity rather than the intramolecular origin. The profiles were divided from their appearance into three portions: the main melting band at about average melting temperature, and peak groups on its low- and high-temperature shoulders. The variety among the species is mainly found in the third group, the most GC-rich portion. The DNA component, which indicates such high compositional variation among different mammalian DNAs, contains probably highly repeated sequences, which are not generally transcribed for structural proteins. Low natural selection pressure on these sequences might have produced, they assumed, the compositional variety. By introducing a quantitative parameter,* which characterizes the similarity of melting profiles, they derived a phylogenetic tree for the mammalians examined.

A specific structural arrangement within a train of the genes coded for ribosomal RNAs[100,101,231] or histone molecules[103] has been studied by the high-resolution melting technique together with electron microscopic observations. These genes are known to have multiple tandem arrangement where the gene sequence alternates with the spacer sequence.

The melting profiles of the chromosomal ribosomal-DNA of somatic cells and of the ribosomal-DNA in oocytes of *Xenopus laevis* were investigated.[101,231] The latter is amplified about 1000-fold compared to the former. The profiles are similar in shape and consist of two main melting bands. The low-temperature band is assigned to the melting of the 18S and 28S gene sequence, and the high-temperature band to the spacer sequence. The chromosomal r-DNA, however, was found to be more stable than the

* This parameter is simply expressed by the mean difference between the melting profiles of the i-th and j-th species as

$$p_{ij} = \int_{60}^{85} |A_i(T) - A_j(T)| dT$$

where A_i (T) is the normalized hyperchromicity-temperature dependence defined by the i-th melting curve. The integral is carried out to cover the major regions of the curve.[85]

amplified r-DNA, the origin of which is accounted for as the 5-methylation of cytocin residues in the former DNA.[101]

The ribosomal DNAs of *X. mulleri* were compared with that of *X. laevis*.[100] The melting profiles exhibit a similar complexity with two melting bands as mentioned above but quantitatively, about half of the spacer sequence of the r-DNA is found to move into the low-temperature band in the case of *X. mulleri*.

A similar tandem repetition of genes was studied on the histone genes of the sea urchin.[103] The DNA has five histone coding sequences alternately with the spacer sequence which is repeated several hundred times. The melting profile exhibits two main melting bands of almost the same size which are fairly sharp and distinctly separated by about an 8°C temperature interval. The higher temperature band is assigned to the melting of the histone coding sequences because they have been known to have relatively high GC composition corresponding to its Tm. The intermediate state where only AT-rich spacer sequences have been melted is clearly exhibited by electron microscopy; a quantitative agreement was demonstrated between the sizes of the GC-rich region and the histone molecules.

A tandem repetition of the genes and its contrasted stability difference between the sequences of the structure coded and of the spacer, as observed in the several studies mentioned above, seems to offer a number of promising applications of the high-temperature-resolution technique. The electron microscopic observation will play a complementary role with its high-positional resolution.

2. Detection of Defects and Mispairing in DNA

Since the helix stability of a free chain end is relatively weak[10,232] and the effect extends beyond several hundred bases from it,[62] a defect such as single-chain scission or unmatched bases alters the melting profile to some extent. This provides a useful tool for examining the degree of base-pair matching of refolded DNAs.[101] The result with the refolded form of homologous DNAs gives information about the complexity of base sequence which produces an accidental mismatching in the refolding. On the other hand, the degree of similarity of base sequences, the extent of genetic homology, can be estimated with the heteroduplex of heterologous DNAs. This kind of application of the melting was made, mostly in conjunction with refolding or the Cot analysis, with the DNAs of mitochondria,[90] *Xenopus* ribosomal,[100,101] and mouse satellite.[112]

The degree of homology in the base sequences of two mitochondrial DNAs from different species of *X. laevis* and *X. mulleri* was examined.[95] The stability of the heteroduplexes which were prepared by annealing under all possible combinations of separated strands of the mitochondrial DNAs were analyzed and the analysis led to the following conclusion: (1) about 30% of the sequences in these mitochondrial DNAs do not interact, indicating that about half of all bases in these sequences differ in their thermal stabilities; (2) about 50% of the DNAs form a heteroduplex with an average of 27% mismatched bases; and (3) 20% of the DNAs form a heteroduplex with an average of 6% mismatched bases.

A similar experiment was done for the DNA from *Chlamydomonas reinhardi* which indicates two melting components.[76] The melting profile of the renatured DNA agrees well with that of the native DNA, indicating that the DNA is in a good register and that the two components have unique base sequences.

Another interesting example was given by the ribosomal DNA of *Tetrahymena*, which has a giant palindrome sequence over some 10^4 bases.[102] The two polynucleotide strands of this DNA are self-complementary so that each of the completely unfolded single strands at high temperature rapidly refolds by itself with first-order kinetics by cooling the solution. Native DNAs reveal a melting curve with at least six peaks. The refolded DNA by rapid cooling, where intermolecular reassociation is prohibited and

only the intramolecular folding at the center of the palindrome symmetry occurs, exhibits the same pattern of the melting peaks with the same melting temperatures but with different heights in some peaks. The results clearly indicate that the matching between each half of the palindrome sequence in one strand should be excellent in most part of this DNA.[102]

3. Mapping of Base Pairs

Several techniques have been exploited for the sequence determination of the arrangement of cooperatively melting regions and local base compositions. The melting-refolding method has been described in Section V. The reconstruction method by detailed comparison of melting profiles measured for different sets of restriction fragments was applied to the mapping of the fd phage DNA before the establishment of its base sequence (Section IV). The result shows fairly good agreement with the map calculated with reference to the sequence disclosed recently.

A new idea which may be called the solvent perturbation method has been presented by Azbel.[146,148] The practical usefulness of the method under a limited experimental condition and resolution remains to be demonstrated in the future.

Grachev and Perelroyzen[77] studied, with their newly developed microspectrophotometric device, a fragment of T7 DNA with 1000 base pairs containing four early promoters. It was shown that the lowest melting region is involved in these early promoters.

4. Location of Specific Binding of Ligands

A moderately long-range correlation in the double helix stability provides a means to probe the specific binding of a molecule which stabilizes or destabilizes the double helical structure at the site of binding.[37,52] Polyamines[233] and polymers of basic amino acids[58] have been known to alter the Tm of the DNA and to exhibit a bimodal melting profile conforming to the stoichiometry of binding. A qualitative examination on the binding of five major histone fractions from calf thymus to rat thymus DNA has been carried out by observing progressive stages of the melting of these complexes.[50] The results in 3.6 *M* urea at low ionic strength indicate that the complexes of the five histone fractions are distinctive with respect to (1) the number of complexes formed by the fraction and the weight distribution among these complexes, (2) the apparent binding strength, and (3) the complexing efficiency found as F1 > F2b > F3 ≃ F2a1 ≃ F2a2 on a weight basis. A stoichiometric relationship is found to be held as [Arg] + [Lys] = DNA phosphate, except for the F1 complex.[50] The change which is produced by the F1 component of calf thymus histone and which appears in some specific peaks in the melting profile of the λ DNA has been examined.[70] The peaks affected by the complex formation indicate the binding site to be in the right half of the λ genom.

The melting of rat liver chromatin was investigated in which the effects of histone and nonhistone proteins were revealed as a fine structure in the melting process.[86] The major part of the melting is situated at temperatures higher than in a pure DNA which is distinctly attributed to the contribution by nucleosome. The chromatin nonhistone protein-DNA complex destabilizes the DNA double strand; hence the melting appears at a temperature lower than in a DNA. The specific extraction of these proteins changes the Tm of the corresponding melting peaks according to their stabilizing or destabilizing effect. Staynov[238] analyzed theoretically the melting of DNA stripped of non-histone proteins and H1, and showed that explicit structural conclusions can be drawn from the observed melting curve.

The effect of enzymatically bound 4-hydroxy aminoquinoline 1-oxide (4HAQO) to the DNA has been studied by the melting measurement for the purpose of disclosing

the binding characteristic of this potent carcinogen.[234] In the melting profile of the λ DNA, the binding of 4HAQO obscures the melting structure where peaks tend to broaden and fuse with neighboring ones. The result indicates, together with the result of synethic DNAs, that the binding is base-sequence-dependent and affects the stability of a fairly long double helical stretch.

ACKNOWLEDGMENTS

The authors take pleasure in acknowledging the generous assistance and advice given by Drs. O. Gotoh, H. Tachibana, and S. Ueno-Nishio during the preparation of this review. We would like to thank the participants to the workshop on the high-resolution studies on the melting of DNA and RNA held on the occasion of the VI International Congress of Pure and Applied Biophysics, held on September 9, 1978, in Kyoto, Japan, by whom we were much inspired and who gave many important suggestions. Finally, we should like to express our indebtedness to Dr. Blake and to Drs. Vizard and Ansevin for permission to reproduce their data in some of our figures.

REFERENCES

1. **Marmur, J., Round, R., and Schildkraut, C. L.,** Denaturation and renaturation of deoxyribonucleic acid in *Progress in Nucleic Acid Research and Molecular Biology: An International Series,* Vol. 1, Davidson, J. N. and Cohn, W. E., Eds., Academic Press, New York, 1963, 231.
2. **Zimm, B. H. and Kallenbach, N. R.,** Selected aspects of the physical chemistry of polynucleotides and nucleic acids, *Annu. Rev. Phys. Chem.*, 13, 171, 1962.
3. **Poland, D. and Scheraga, H. A.,** *Theory of Helix Coil Transitions in Biopolymers,* Academic Press, New York, 1970.
4. **Wartell, R. M. and Montroll, E. W.,** Equilibrium denaturation of natural and of periodic synthetic DNA molecules, *Adv. Chem. Phys.*, 22, 129, 1972.
5. **Lazurkin, Yu. S., Frank-Kamenetskii, M.D., and Trifonov, E. N.,** Melting of DNA: its study and application as a research method, *Biopolymers,* 9, 1253, 1970.
6. **Tinoco, I., Jr.,** Nucleic acids, *Annu. Rev. Phys. Chem.*, 15, 371, 1964.
7. **McCarthy, B. J.,** The evolution of base sequence in polynucleotides, in *Progress in Nucleic Acid Research and Molecular Biology: An International Series,* Vol. 4, Davidson, J.N. and Cohn, W. E., Eds., Academic Press, New York, 1965, 129.
8. **Wetmur, J. G. and Davidson, N.,** Kinetics of renaturation of DNA, *J. Mol. Biol.*, 31, 349, 1968.
9. **Britten, R. J. and Kohne, D. E.,** Repeated sequence in DNA, *Science,* 161, 529, 1968.
10. **Kohne, D. E.,** Evolution of higher organism DNA, *Q. Rev. Biophys.*, 33, 327, 1970.
11. **Tinoco, I.,** Hypochromism in polynucleotides, *J. Am. Chem. Soc.*, 82, 4785, 1960.
12. **Tinoco, I.,** Optical and other electronic properties of polymers, *J. Chem, Phys.*, 33, 1332, 1960; erratum, *J. Chem. Phys.*, 34, 1967, 1961.
13. **Marmur, J. and Doty, P.,** Determination of the base composition of DNA from its thermal denaturation temperature, *J. Mol. Biol.*, 5, 109, 1962.
14. **DeLey, J.,** Compositional nucleotide distribution and the theoretical prediction of homology in bacterial DNA, *J. Theor. Biol.*, 22, 89, 1969.
15. **Gasser, F. and Mandel, M.,** DNA base composition of the genus *Lactobacillus, J. Bacteriol.*, 96, 580, 1968.
16. **Mandel, M. and Marmur, J.,** Use of ultraviolet-absorbance temperature profile for determining the G + C content of DNA, in *Methods in Enzymology,* Vol. 12 (Part B), Grossman, L. and Moldave, K., Eds., Academic Press, New York, 1968, 195.
17. **Owen, R. J., Hill, L. R., and Lepage, S. P.,** Determination of DNA base compositions from melting profiles in dilute buffers, *Biopolymers,* 7, 503, 1969.
18. **Mandel, M., Igambi, L., Bergendahl, J., Dodson, M. L., Jr., and Scheltgen, E.,** Correlation of melting temperature and cesium chloride buoyant density of bacterial DNA, *J. Bacteriol.*, 101, 333, 1970.

19. **Frank-Kamenetskii, M.D.**, Simplification of the empirical relationship between melting temperature of DNA, its GC content and concentration of sodium ion in solution, *Biopolymers*, 10, 2623, 1971.
20. **Blake, R. D. and Lefoley, S. G.**, Spectral analysis of high resolution direct-derivative melting curves of DNA for instantaneous and total base composition, *Biochim. Biophys. Acta*, 518, 233, 1978.
21. **Inman, R. B. and Baldwin, R. L.**, Helix-random coil transition in synthetic DNAs of alternating sequence, *J. Mol. Biol.*, 5, 172, 1962.
22. **Schildkraut, C. and Lifson, S.**, Dependence of the melting temperature of DNA on salt concentration, *Biopolymers*, 3, 195, 1965.
23. **Pohl, F. M.**, Thermodynamics of the helix-coil transition of (dG-dC) oligomers, *Eur. J. Biochem.*, 42, 495, 1974.
24. **Inman, R. B. and Baldwin, R. L.**, Formation of hybrid molecules from two alternating DNA copolymers, *J. Mol. Biol.*, 5, 185, 1962.
25. **Pivec, L., Sponer, J., and Sormova, Z.**, Subunit structure of calf-thymus DNA from absorption curves of thermal denaturation, *Biochim. Biophys. Acta*, 91, 357, 1964.
26. **Pivec, L., Pivocova, H., and Sormova, Z.**, Plurimodal heterogeneity of base composition of DNA isolated from *B. subtilis*, *Biochim. Biophys. Acta*, 213, 343, 1970.
27. **Falkow, S. and Cowie, D. B.**, Intramolecular heterogeneity of the DNA of temperate bacteriophage, *J. Bacteriol.*, 96, 777, 1968.
28. **Yabuki, S., Wada, A., and Uemura, K.**, Automatic recording of the melting curves of nucleic acids, *J. Biochem. (Tokyo)*, 65, 443, 1969.
29. **Yabuki, S., Fuke, M., and Wada, A.**, The fine structures in melting curves of DNA of bacteriophage lambda I, *J. Biochem. (Tokyo)*, 69, 191, 1971.
30. **Bernardi, G., Faures, M., Piperno, G., and Slonimski, P. P.**, Mitochondrial DNAs from respiratory-sufficient and cytoplasmic respiratory-deficient mutant yeast, *J. Mol. Biol.*, 48, 23, 1970.
31. **Gomez, B. and Lang, D.**, Denaturation map of bacteriophage T_7 DNA and direction of DNA transcription, *J. Mol. Biol.*, 70, 239, 1972.
32. **Inman, R. B.**, A denaturation map of the λ-phage DNA molecule determined by electron micrography, *J. Mol. Biol.*, 18, 464, 1966.
33. **Inman, R. B.**, Denaturation maps of the left and right sides of the lambda DNA molecule determined by electron microscopy, *J. Mol. Biol.*, 28, 103, 1967.
34. **Vizard, D. L. and Ansevin, A. T.**, High resolution thermal denaturation of DNA: thermalites of bacteriophage DNA, *Biochemistry*, 15 (4), 741, 1976.
35. **Szybalski, W.**, Effects of elevated temperatures on DNA and on some polynucleotides: denaturation, renaturation and cleavage of glycosidic and phosphate ester bond, in *Thermobiology*, Rose, A. H., Ed., Academic Press, New York, 1967, chap. 4.
36. **Felsenfeld, G. and Miles, H.**, The physical and chemical properties of nucleic acids, *Annu. Rev. Biochem.*, 36, 407, 1967.
37. **Frank-Kamenetskii, M. D. and Lazurkin, Y. S. A.**, Conformational changes in DNA molecules, *Annu. Rev. Biophys. Bioeng.*, 3, 127, 1974.
38. **Steiner, RF. and Beers, R. F., Jr.**, *Polynucleotides*, Elsevier, Amsterdam, 1961.
39. **Michelson, A., Massoulie, J., and Guschbauer, W.**, Synthetic polynucleotides, in *Progress in Nucleic Acid Research and Molecular Biology: An International Series*, Vol. 6, Davidson, J. N. and Cohn, W. E., Eds., Academic Press, New York, 1967, 83.
40. **Wells, R. D. and Watell, R. M.**, The influence of nucleotide sequence on DNA properties, in *Biochemistry of Nucleic Acids*, Vol. 6, Kornberg, H. L., Phillips, D.C., and Burton, K., Eds., University Park Press, Baltimore, 1974, 41.
40a. **Wells, R. D., Blakesley, R. W., Hardies, S. C., Horn, G. C., Larson, J. E., Selsing, E., Burd, J. F., Chan, H. W., and Dodgson, J. B.**, The role of genetic structure in genetic regulation, *CRC Crit. Rev. Biochem.*, 4(3), 305, 1977.
41. **Blake, R. D.**, Polynucleotides, in *Encyclopedia of Polymer Science and Technology*, Suppl. 2, John Wiley & Sons, New York, 1977, 510.
42. **Riesner, D., Römer, R., and Maass, G.**, Thermodynamic properties of the three conformational transitions of ala transfer RNA from yeast, *Biochem. Biophys. Res. Commun.*, 35, 369, 1969.
42a. **Riesner, D. and Römer, R.**, Thermodynamics and kinetics of conformation transition in oligonucleotides and t-RNA, in *Physico-chemical Properties of Nucleic Acids, Vol. 2*, Duchesne, J., Ed., Academic Press, New York, 1973, 237.
43. **Römer, R., Riesner, D., Coutts, S. M., and Maass, G.**, The coupling of conformational transitions in t-RNA from yeast studied by a modified differential absorption technique, *Eur. J. Biochem.*, 15, 77, 1970.
44. **Pavlov, V. M. and Lyubchenko, Yu. L.**, A new method for recording of DNA differential melting curve, *Biopolymers*, 17, 795, 1978.

45. Lyubchenko, Yu. L., Frank-Kamenetskii, M.D., Vologodskii, A. V., Lazurkin, Yu. S., and Gause, G. G., Jr., Fine structure of DNA melting curves, *Biopolymers*, 15, 1019, 1976.
46. Reiss, C., Michel, F., and Gabarro, U., An apparatus for studying the thermal transition of nucleic acids at high resolution, *Anal. Biochem.*, 62, 499, 1974.
47. Vitek, A., Reddy, C., and Pivec, L., Numerical analysis of absorption melting curves of a multiphasic shape by a computer, *Biochim. Biophys. Acta*, 353, 385, 1974.
48. Ansevin, A. T., Vizard, D. L., Brown, B. W., and McConathy, J., High resolution thermal denaturation of DNA. I. Theoretical and practical considerations for the resolution of thermal subtransitions, *Biopolymers*, 15, 153, 1976.
49. Gotoh, O., Husimi, Y., Yabuki, S., and Wada, A., Hyperfine structure in melting profile of bacteriophage lambda, *Biopolymers*, 15, 655, 1976.
50. Ansevin, A. T. and Brown, B. W., Specificity in the association of histones with deoxyribonucleic acid. Evidence from thermal denaturation profiles, *Biochemistry*, 10, 1133, 1971.
51. Michel, F., Histeresis and partial irreversibility of denaturation of DNA as a means of investigating the topology of base distribution constraints. Application to a yeast ϱ (petit) mitochondrial DNA, *J. Mol. Biol.*, 89, 305, 1974.
52. Reiss, C. and Arpa-Gabarro, T., Thermal transition spectroscopy. A new tool for submolecular investigation of biological macromolecules, in *Progress in Molecular and Subcellular Biology*, Vol. 5, Hahn, F. E., Ed., Springer-Verlag, Berlin, 1977, 1.
53. Yabuki, S., Gotoh, O., and Wada, A., Fine structures in denaturation curves of bacteriophage lambda DNA. Their relation to the intramolecular heterogeneity in base composition, *Biochim. Biophys. Acta*, 395, 258, 1975.
54. Tachibana, H., Salt concentration dependence of the fine structure of melting profiles of ϕX174 DNA, unpublished, 1978.
55. Riesner, D., private communication, 1978.
56. Felsenfeld, G., Analysis of temperature-dependent absorption spectra of nucleic acid, in *Procedures in Nucleic Acid Research*, Vol. 2, Cantoni, G. L. and Davis, D. R., Eds., Harper & Row, New York, 1971, 233.
57. Felsenfeld, G., Sandeen, G., and Von Hippel, P. H., The destabilizing effect of ribonuclease on the helical DNA structure, *Proc. Natl. Acad. Sci. U.S.A.*, 50, 644, 1963.
58. Tsuboi, M., Matsuo, K., and Ts'o, P.O.P., Interaction of poly-L-lysine and nucleic acids, *J. Mol. Biol.*, 15, 256, 1966.
59. Shin, T. Y. and Bonner, J., Thermal denaturation and template properties of DNA complex with purified histone fractions, *J. Mol. Biol.*, 48, 469, 1970.
60. Wada, A., Tachibana, H., Gotoh, O., and Takanami, M., Long range homogeneity of physical stability in double stranded DNA, *Nature*, 263, 439, 1976.
61. Tachibana, H., Wada, A., Gotoh, O., and Takanami, M., Location of the cooperative melting regions in bacteriophage fd DNA, *Biochim. Biophys. Acta*, 517, 319, 1978.
62. Wada, A., Ueno, S., Tachibana, H., and Husimi, U., Stability mapping along the DNA double strand and its relation to the genetic map, *J. Biochem. (Tokyo)*, 85, 827, 1979.
63. Lindahl, T. and Nyberg, B., Rate of depurination of native DNA, *Biochemistry*, 11, 3610, 1972.
64. Lindahl, T. and Karlstrom, O., Heat induced depyrimidination of DNA in neutral solution, *Biochemistry*, 12, 5151, 1973.
65. Lindahl, T. and Nyberg, B., Heat induced depyrimidination of cytosine redidues in DNA, *Biochemistry*, 13, 3415, 1974.
66. Lazurkin, Yu. S., Lyubchenko, Yu. L., Pavlov, V. M., Frank-Kamenetskii, M. D., and Berestetskaya, I. V., On the parameters of DNA melting curves in the low Na^+ ion concentration range, *Biopolymers*, 14, 1551, 1975.
67. Riesner, D., private communication, 1978.
68. Gabarro, J., Numerical analysis of thermal denaturation of biological macromolecules, private communication, 1978.
69. Pivec, L., Horska, K., Vitek, A., and Doskoiel, J., Plurimodal distribution of base composition in DNA of some higher plants, *Biochim. Biophys. Acta*, 340, 199, 1974.
70. Bram, S., Butler-Brown, G., Bradbury, E. M., Baldwin, J., and Reiss, C., Chromatin, neutron and X-ray diffraction studies, and high resolution melting of DNA-histone complexes, *Biochemie*, 56, 987, 1974.
71. Aikyama, C., Gotoh, O., and Wada, A., Spectral analysis on the melting fine structure of λ-DNA and T_2 DNA, *Biopolymers*, 16, 427, 1977.
72. Gotoh, O., Yabuki, S., and Wada, A., Salt-concentration dependence of melting profile of lambda phage DNAs: evidence for long-range interactions and pronounced end effects, *Biopolymers*, in press.

73. **Inman, R. B. and Bertani, G.,** Heat denaturation of P2 bacteriophage DNA: compositional heterogeneity, *J. Mol. Biol.*, 44, 533, 1969.
74. **Gotoh, O.,** Fine Structures in Optical Melting Profiles of Natural DNAs, Ph.D. thesis, University of Tokyo, 1978.
75. **Jakovcic, S., Casey, J., and Rabinowitz, M.,** Sequence homology between mitochondrial DNAs of different eukaryotes, *Biochemistry*, 14, 2043, 1975.
76. **Wells, R. and Sager, R.,** Denaturation and renaturation kinetics of chlorophast DNA from *Chlamydomonas reinhardi*, *J. Mol. Biol.*, 58, 611, 1971.
77. **Grachev, M. A. and Perelroyzen, M. P.,** Measurement of the differential melting profile of a promotor containing fragment of T, DNA by means of a microspectrophotometer, *Nucleic Acid Res.*, 5, 2557, 1978.
78. **Lyubchenko, Y. L., Vologodskii, A. V., and Frank-Kamenetskii, M. D.,** Direct comparison of theoretical and experimental melting profiles for RFII ϕX174 DNA, *Nature*, 271, 28, 1978.
79. **Vizard, D. L., White, R. A., and Ansevin, A. T.,** Comparison of theory to experiment for DNA-thermal denaturation, *Nature*, 275, 250, 1978.
80. **Wada, A., Tachibana, H., Ueno, S., Husimi, Y., and Machida, Y.,** Melting fine structure of DNA fragments of known base sequence from ϕX174, *Nature*, 269, 352, 1977.
81. **Mayer, F., Lotz, W., and Lang, D.,** Electron microscope study of length and partial denaturation of *Rhizobium bacteriophage* DNA, *J. Virol.*, 11, 946, 1973.
82. **Quetier, F. and Guille, E.,** Studies on plant DNAs. I. Extraction, fractionation and analytical thermal denaturation, *Arch. Biochem. Biophys.*, 124, 1, 1968.
83. **Pivec, L., Stokrova, J., and Sormova, Z.,** Plurimodal heterogeneity of base composition of calf thymus DNA, *Biochim. Biophys. Acta*, 272, 179, 1972.
84. **Gruenwedel, D. W.,** Salt effects on the denaturation of DNA. A calorimetric investigation of the transition enthalpy of calf thymus DNA in Na_2SO_4 solutions of varying ionic strength, *Biochim. Biophys. Acta*, 340, 16, 1974.
85. **Guttman, T., Vitek, A., and Pivec, L.,** High resolution thermal denaturation of mammalian DNAs, *Nucleic Acid Res.*, 4, 285, 1977.
86. **Defer, N., Kitzis, A., Kruh, J., Brahms, S., and Brahms, J.,** Effect of non-histone proteins on thermal transition of chromatin and of DNA, *Nucleic Acid Res.*, 4, 2293, 1977.
87. **Yabuki, S., Tagashira, Y., and Wada, A.,** Compositional heterogeneity of rat liver mitochondrial DNA, *Gunma J. Liberal Arts Sci.*, 6, 55, 1972.
88. **Huget, T. and Jouanin, L.,** The heterogeneity of wheat nuclear DNA, *Biochim. Biophys. Acta*, 262, 431, 1972.
89. **Faye, G., Fukuhara, H., Grandchamp, C., Lazowska, J., Michel, F., Casey, J., Getz, G. S., Locker, J., Rabinowitz, M., Bolotin-Fukuhara, M., Coen, D., Deutsch, J., Dujon, B., Netter, P., and Slonimski, P. P.,** Mitochondrial nucleic acids in the petite colonic mutants: deletion and repetition of genes, *Biochimie*, 55, 779, 1973.
90. **Michel, F., Lazowska, J., Faye, G., Fukuhara, H., and Slonimski, P. P.,** Physical and genetic organization of petite and grande yeast mitochondrial DNA. III. High resolution melting and reassociation studies, *J. Mol. Biol.*, 85, 411, 1974.
91. **Michaelis, G., Michel, F., Lazowska, J., and Slonimski, P. P.,** Recombined molecules of mitochondrial DNA obtained from cross between cytoplasmic petite mutants of *Saccharomyces cerevicial*. The stoichiometry of partial DNA repeats within the recombined molecule, *Mol. Gen. Genet.*, 149, 125, 1976.
92. **Michel, F., Grandchamp, C., and Dujon, B.,** Genetic and physical characterization of a segment of yeast mitochondrial DNA involved in the control of genetic recombination, *Mol. Gen. Genet.*, submitted.
93. **Dujon, B. and Michel, F.,** Genetic and physical characterization of a segment of the mitochondrial DNA involved in the control of genetic recombination, in *The Genetic Function of Mitochondrial DNA*, Saccone, C. and Kroon, A.M., Eds., Elsevier, Amsterdam, 1976, 175.
94. **Yabuki, S.,** Analysis of Fine Structures in Thermal Denaturation and Renaturation Profiles of DNA, Ph.D. Thesis, University of Tokyo, 1978.
95. **Dawid, I.B.,** Evolution of mitochondrial DNA sequence in *Xenopus*, *Dev. Biol.*, 29, 139, 1972.
96. **Yabuki, S., Gotoh, O., and Wada, A.,** Hysteresis of DNA denaturation and fine structure in renaturation profile from partially denatured states, in Proc. 3rd Taniguchi Symp. Biophysics Branch, Kotani, M., Ed., Kyoto, 1977, 273.
97. **Pochon, F., Massoulié, J., and Michelson, A.M.,** Polynucleotides. VII. Les DNA satellites du Thymus de veau et "Poly d(A-T) de Crabe", *Biochim. Biophys. Acta*, 119, 249, 1966.
98. **Skowronski, J., Furtak, K., Klysik, J., Panusz, H., and Pluciennicak, A.,** The 1360 b.p. long basic repeat unit of calf satellite I DNA contains GC rich nucleus of about 140 b.p., *Nucleic Acid Res.*, 5, 4077, 1978.

99. **Mazrimas, J. A. and Hatch, F. T.,** Similarity of satellite DNA properties in the order rodentia, *Nucleic Acid Res.*, 4, 3215, 1977.
100. **Brown, D. D., Wensink, P. C., and Jordan, E.,** A comparison of the ribosomal DNA's of *Xenopus laevis* and *Xenopus mulleri:* The evolution of tandem genes, *J. Mol. Biol.*, 63, 57, 1972.
101. **Dawid, I. B., Brown, D. D., and Reeder, R. H.,** Composition and structure of chromosomal and amplified ribosomal DNA's of *Xenopus laevis, J. Mol. Biol.*, 51, 341, 1970.
102. **Karrer, K. M. and Gall, J. G.,** The macromolecular ribosomal DNA of *Tetrahymena pyriformis* is a palindrome, *J. Mol. Biol.*, 104, 421, 1976.
103. **Portmann, R., Schaffner, W., and Birnstiel, M.,** Partial denaturation mapping of cloned histone DNA from the sea urchin *Psammechinus miliaris, Nature*, 264, 31, 1976.
104. **Riou, G. and Paoletti, C.,** Preparation and properties of nuclear and satellite DNA of *Trypanosoma cruzi, J. Mol. Biol.*, 28, 377, 1969.
105. **Steinert, M. and Van Assel, S.,** Base composition heterogeneity in kinetoplast DNA from four species of hemoflagellates, *Biochem. Biophys. Res. Commun.*, 61, 1259, 1974.
106. **Ueno, S.,** Statistical Thermodynamic Analysis of the Thermal Denaturation of DNA, Ph.D. Thesis, University of Tokyo, 1978.
107. **Frank-Kamenetskii, M. D. and Vologodskii, A. V.,** The nature of the fine structure of DNA melting curves, *Nature*, 269, 729, 1977.
108. **Ueno, S., Tachibana, H., Husimi, Y., and Wada, A.,** "Thermal stability" maps for several double-stranded DNA fragments of known sequence, *J. Biochem. (Tokyo)*, 84, 917, 1978.
109. **Skalka, A., Burgi, E., and Hershey, A.,** Segmental distribution of nucleotides in the DNA of bacteriophage lambda, *J. Mol. Biol.*, 34, 1, 1968.
110. **Yamagishi, H.,** Nucleotide distribution in the DNA of *E. coli, J. Mol. Biol.*, 49, 603, 1970.
111. **Walker, P. M. B.,** The specificity of molecular hybridization in relation to studies on higher organism, in *Progress in Nucleic Acid Research and Molecular Biology: An International Series*, Vol. 9, Davidson, J. N. and Cohn, W. E., Eds., Academic Press, New York, 1969, 301.
112. **Walker, P. M. B.,** Repetitive DNA of higher organism, *Prog. Biophys. Mol. Biol.*, 23, 145, 1971.
113. **Felsenfeld, G. and Sandeen, G.,** The dispersion of the hyperchromic effect in thermally induced transitions of nucleic acids, *J. Mol. Biol.*, 5, 587, 1962.
114. **Fresco, J. R., Klotz, L. C., and Richards E. G.,** A new spectroscopic approach to the determination of helical secondary structure in ribonucleic acids, in *Cold Spring Harbor Symposia on Quantitative Biology*, Vol. 28, Cold Spring Harbor Laboratory, Cold Spring Harbor, N.Y., 1963, 83.
115. **Felsenfeld, G. and Hirschman, S. Z.,** A neighbor interaction analysis of the hypochromism and spectra of DNA, *J. Mol. Biol.*, 13, 407, 1965.
116. **Hirschman, S. Z., Gellert, M., Falkow, S., and Felsenfeld, G.,** Spectral analysis of the intermolecular heterogeneity of λ DNA, *J. Mol. Biol.*, 28, 469, 1967.
117. **Hirschman, S. Z. and Felsenfeld, G.,** Determination of DNA composition and concentration by spectral analysis, *J. Mol. Biol.*, 16, 347, 1966.
118. **Tachibana, H., Gotoh, O., and Wada, A.,** unpublished, 1978.
119. **Blake, R. D. and Haydock, P. V.,** High resolution melting of DNA. Extenuating effects of ionic strength, private communication, 1978.
120. **Wells, R. D., Larson, J. E., Grant, R. C., Cantor, C. R., and Shortle, B.,** Physicochemical studies on polydeoxynucleotides containing defined repeating nucleotide sequences, *J. Mol. Biol.*, 54, 465, 1970.
121. **Ratliff, R. L., Williams, D. L., Hayes, F. N., Martinez, E. L., Jr., and Smith, D. A.,** Preparation and properties of repeating sequence polymer d(A-A-T)$_n$ d(T-A-A)$_n$', *Biochemistry*, 12, 5005, 1973.
122. **Dove, W. F. and Davidson, N.,** Cation effects on the denaturation of DNA, *J. Mol. Biol.*, 5, 467, 1962.
123. **Berestetskaya, I.V., Frank-Kamenetskii, M. D., and Lazurkin, Yu. S.,** Effect of ionic conditions on DNA melting curve parameters, *Biopolymers*, 13, 193, 1974.
124. **Record, M. T., Jr.,** Effects of Na^+ and Mg^{2+} ions on the helix-coil transition of DNA, *Biopolymers*, 14, 2137, 1975.
125. **Oliver, A. L., Wartell, R. M., and Ratliff, R. L.,** Helix-coil transition of d(A)$_n$ d(T)$_n$' d(A-T)$_n$ d(A-T)$_n$ and D(A-A-T)$_n$ d(A-A-T)$_n$. Evaluation of parameters governing DNA stability, *Biopolymers*, 16, 1115, 1977.
126. **Riley, M., Maling, B., and Chamberlin, M. J.,** Physical and chemical characterization of two and three stranded AT and AU homopolymer complex, *J. Mol. Biol.*, 20, 359, 1966.
127. **Blake, R. D.,** Helix-coil equilibria of poly (rA)·poly (rU), *Biophys. Chem.*, 1, 24, 1973.
128. **Elson, E. L., Scheffler, I. E., and Baldwin, R. L.,** Helix-formation by d(TA) oligomers. III. Electrostatic effect, *J. Mol. Biol.*, 54, 401, 1970.
129. **Gruenwedel, D. W.,** Salt effects on the denaturation of DNA. A calorimetric study of the helix-coil conversion of the alternating copolymer poly [d(A-T)], *Biochim. Biophys. Acta*, 395, 246, 1975.

130. **Burd, J. F., Wartell, R. M., Dodgson, J. B., and Wells, R. D.,** Transmission of stability (telestability) in DNA. Physical and enzymatic studies on the duplex block polymer $d(C_{15}A_{15})$ $d(T_{15}G_{15})$, *J. Biol. Chem.*, 250, 5109, 1975.
131. **Burd, J. F., Lorson, J. E., and Wells, R. D.,** Further studies on telestability in DNA, *J. Biol. Chem.*, 250, 6002, 1975.
132. **Wartell, R. M. and Burd, J. F.,** Evidence for long-range interactions in DNA. Analysis of melting curves of block polymers, $d(C_{15}A_{15})$ $d(T_{15}G_{15})$, $d(C_{20}A_{15})$ $d(T_{15}G_{20})$ and $d(C_{20}A_{10})$ $d(T_{10}G_{20})$, *Biopolymers*, 15, 1461, 1976.
133. **Inman, R. B. and Baldwin, R. L.,** Helix-random coil transition in DNA homopolymer pairs, *J. Mol. Biol.*, 8, 452, 1964.
134. **Fuke, M., Wada, A., and Tomizawa, J-I.,** Denaturation at the right-hand end of the DNA molecule of lambda bacteriophage, *J. Mol. Biol.*, 51, 255, 1970.
135. **Lewin, S. and Pepper, D.,** Action of urea of calf thymus DNA, *Arch. Biochem. Biophys.*, 112, 243, 1965.
136. **Venner, H. and Zimmer, C. H.,** Studies on nucleic acids. VIII. Changes in the stability of DNA secondary structure by interaction with divalent metal ions, *Biopolymers*, 4, 321, 1966.
137. **Shin, Y. A. and Eichhorn, G. L.,** Interactions of metal ions with polynucleotides and related compounds. VI. The reversible unwinding and rewinding of DNA Zn^{++} ions through temperature manipulation, *Biochemistry*, 7, 1062, 1968.
138. **Eichhorn, G. L. and Shin, Y.A.,** Interaction of metal ions with polynucleotides and related compounds. XII. The relative effect of various metal ions on DNA helicity, *J. Am. Chem. Soc.*, 90, 7323, 1968.
139. **Daune, M., Dekker, C. A., and Shachan, H. K.,** Complexes of silver ion with natural and synthetic polynucleotides, *Biopolymers*, 4, 51, 1966.
140. **Wilhelm, F. X. and Duane, M.,** Interaction des ions metalliques avec le DNA. III. Stabilite et configuration des complexes Ag-DNA, *Biopolymers*, 8, 121, 1969.
141. **Hiai, S.,** Effects of cupric ions on thermal denaturation of nucleic acids, *J. Mol. Biol.*, 11, 672, 1965.
142. **Eichhorn, G. L. and Clark, P.,** Interaction of metal ions with polynucleotides and related compounds. V. The unwinding and rewinding of DNA strands under the influence of Cu^{2+} ions, *Proc. Natl. Acad. Sci. U.S.A.*, 53, 586, 1965.
143. **Luck, G. and Zimmer, Ch.,** Thermische Schmerzen and optische Rotationdispersion von DNA Hg^{+} Komplexen, *Eur. J. Biochem.*, 18, 140, 1971.
144. **Gotoh, O., Wada, A., and Yabuki, S.,** The effect of heavy metal ions on the denaturation characteristics of phage lambda DNA, *Rep. Prog. Polym. Phys. Jpn.*, 16, 661, 1973.
145. **Melchior, W. B., Jr. and Von Hippel, P. H.,** Alteration of the relative stability of dA·dT and dG·dC base pairs in DNA, *Proc. Natl. Acad. Sci. U.S.A.*, 70, 298, 1973.
146. **Azbel, M. Ya.,** DNA sequencing and melting curve, *Proc. Natl. Acad. Sci. U.S.A.*, 76, 101, 1979.
147. **Azbel, M. Ya.,** Random two-component one-dimensional Ising model for heteropolymer melting, *Phys. Rev. Lett.*, 31, 589, 1592E, 1973.
148. **Azbel, M. Ya.,** private communication, 1978.
149. **Helmkamp, G. K. and Ts'o, P. O. P.,** The secondary structures of nucleic acids in organic solvent, *J. Am. Chem. Soc.*, 83, 138, 1961.
150. **Schmidt, R. L. and Boyle, J. A.,** Intensity fluctuation spectroscopy of DNA. I. Temperature profile of bacteriophage N1 DNA, *Biopolymers*, 16, 317, 1977.
150a. **Schmidt, R. L., Whitehorn, M. A., and Mayo, J. A.,** Intensity fluctuation spectroscopy of DNA. II. Temperature profile of bacteriophage ϕ29-DNA, *Biopolymers*, 16, 327, 1977.
151. **Palecek, E.,** Premelting changes in DNA conformation, in *Progress in Nucleic Acid Research and Molecular Biology: An International Series*, Vol. 18, Davidson, J. N. and Cohn, W. E., Eds., Academic Press, New York, 1976, 151.
152. **Miyazawa, Y. and Thomas, C. A.,** Nucleotide composition of short segments of DNA molecules, *J. Mol. Biol.*, 11, 223, 1965.
153. **Tachibana, H., Hayashi, H., and Wada, A.,** in preparation, 1978.
154. **Studier, F. W.,** Effects of the conformation of single-stranded DNA on renaturation and aggregation, *J. Mol. Biol.*, 41, 199, 1969.
155. **Spatz, H. C. and Crothers, D. M.,** The rate of DNA unwinding, *J. Mol. Biol.*, 42, 191, 1969.
156. **Hoff, A. J. and Ross, A. L. M.,** Hysteresis of denaturation of DNA in the melting range, *Biopolymers*, 11, 1289, 1972.
157. **Yabuki, S., Gotoh, O., and Wada, A.,** A model for molecular mechanism of DNA renaturation from partially denatured states, *Rep. Prog. Polym. Phys. Jpn.*, 18, 619, 1975.
158. **Montroll, E. W. and Goel, N. S.,** Denaturation and renaturation of DNA. I. Equilibrium statistics of copolymeric DNA, *Biopolymers*, 4, 855, 1966.
159. **Yabuki, S., Gotoh, O., Sakakibara, Y., and Wada, A.,** in preparation, 1980.

160. **Yonekawa, H., Gotoh, O., Motohashi, J-I., and Tagashira, Y.**, Positioning of the A·T rich regions in rat mitochondrial DNA by electron microscopy and analysis of the hysteresis of denaturation, *Biochim. Biophys. Acta*, 521, 510, 1978.
161. **Reiss, C.**, private communication, 1978.
162. **Lazowska, J., Jacq, C., and Slonimski, P. P.**, Fine structure map constructed by electron microscopy and restriction endonucleases of the mitochondrial DNA segment conferring erythromycin resistance, in *The Genetic Function of Mitochondrial DNA*, Saccone, C., and Kroon, A. M., Eds., Elsevier, Amsterdam, 1976, 325.
163. **Takahaski, H.**, Eine einfache Methode zur Behandlung der statistischen Mechanik eindimensionaler Substanzen, *Proc. Phys. Math. Soc. Jpn.*, 24, 60, 1942; as cited in **Lieb, E. H. and Mattis, D. C.**, Eds., *Mathematical Physics in One-Dimension*, Academic Press, New York, 1966, 5.
164. **Van Hove, L.**, Sur L'Inegrale de Configuration pour les Systemes de Particules a une dimension, *Physica*, 16, 137, 1950.
165. **Landau, L. and Lifschitz, E.**, *Statistical Physics*, Oxford University Press, Oxford, 1958.
166. **Kac, M., Uhlenbeck, G. E., and Hemmer, P. C.**, On the Van der Waals theory of the vapor-liquid equilibrium. I. Discussion of a one-dimensional model, *J. Math. Phys. (N.Y.)*, 4, 216, 1963.
167. **Jacobson, H. and Stockmayer, W. H.**, Intramolecular reaction in polycondensation. I. Theory of linear systems, *J. Chem. Phys.*, 18, 1600, 1950.
168. **Fisher, M. E.**, Effect of excluded volume on phase transition in biopolymers, *J. Chem. Phys.*, 45, 1469, 1966.
169. **Poland, D. and Sheraga, H. A.**, Phase transition in one dimension and the helix-coil transition in polyamino acids, *J. Chem. Phys.*, 45, 1465, 1966.
170. **Poland, D. and Scheraga, H. A.**, Occurrence of a phase transition in nucleic acid models, *J. Chem. Phys.*, 45, 1464, 1966.
171. **Appliquist, J.**, Higher order phase transitions in two stranded macromolecules, *J. Chem. Phys.*, 50, 600, 1969.
172. **Crothers, D. M.**, Calculation of melting curves of DNA, *Biopolymers*, 6, 1391, 1968.
173. **Zimm, B. H.**, Theory of "melting" of the helical form in double chains of the DNA type, *J. Chem. Phys.*, 33, 1349, 1960.
174. **Applequist, J. and Damle, V.**, Thermodynamics of the helix-coil equilibrium in oligoadenylic acid from hypochromicity studies, *J. Am. Chem. Soc.*, 87, 1450, 1965.
175. **Ozaki, M., Tanaka, M., and Teramoto, E.**, Dependence of the transition temperatures of DNA molecules upon their base compositions, *J. Phys. Soc. Jpn.*, 18, 551, 1963.
176. **Lifson, S.**, Theory of the helix-coil transition in DNA considered as a copolymer, *Biopolymers*, 1, 25, 1963.
177. **Lifson, S. and Allegra, G.**, On the theory of order-disorder transition and copolymer structure of DNA, *Biopolymers*, 2, 65, 1964.
178. **Kawai, Y., Ozaki, M., Tanaka, M., and Teramoto, E.**, Theory of helix-coil transition of DNA molecules, *J. Phys. Soc. Jpn.*, 20, 1457, 1965.
179. **Crothers, D. M., Kallenbach, N. R., and Zimm, B. H.**, The melting transition of low molecular weight DNA: theory and experiment, *J. Mol. Biol.*, 11, 802, 1965.
180. **Reiss, H., McQuarric, D. A., McTague, J. P., and Cohen, E. R.**, On the melting of copolymeric DNA, *J. Chem. Phys.*, 44, 4567, 1966.
181. **Lehman, G. W.**, Thermal properties of linearly associated systems with random elements: helix-coil transition in DNA, in *Conf. on Statistical Mechanics and Statistical Thermodynamics*, Bak, T. A., Ed., W. A. Benjamin, New York, 1967, 204.
182. **Vedenov, A. A., Dykhne, A. M., Frank-Kamenetskii, A. D., and Frank-Kamenetskii, M. D.**, A contribution to the theory of helix-coil transition in DNA, *Mol. Biol. (Moscow)*, 1, 272, 1967.
183. **Lehman, G. W. and McTague, J. P.**, Melting of DNA, *J. Chem. Phys.*, 49, 3170, 1968.
184. **Tong, B. Y. and Tong, S. Y.**, Phase transfer theory and its application to long chain molecules: DNA, *J. Chem. Phys.*, 54, 1317, 1971.
185. **Tong, B. Y. and Battersby, S. J.**, Melting fine structure of ϕX-174 DNA and its fragments. A theoretical study, *Biopolymers*, 17, 2933, 1978.
186. **Leung, M., Choo, F. C., and Tong, B.Y.**, Applications of modified Ising model to the helix-coil transition of DNA molecules, *Biopolymers*, 16, 1233, 1977.
187. **Crothers, D. M. and Kallenbach, N. R.**, On the helix-coil transition in heterogeneous polymers, *J. Chem. Phys.*, 45, 917, 1966.
188. **Frank-Kamenetskii, M. D. and Frank-Kamenetskii, A. D.**, Theory of the helix-coil transition for the case of double-stranded DNA, *Mol. Biol. (Moscow)*, 3, 295, 1969.
189. **Lukashin, A.V., Vologodskii, A. V., and Frank-Kamenetskii, M. D.**, Comparison of different theoretical descriptions of helix-coil transition in DNA, *Biopolymers*, 15, 1841, 1976.
190. **Fixman, M. and Freire, J. J.**, Theory of DNA melting curves, *Biopolymers*, 16, 2693, 1977.

191. **Poland, D.,** Recursion relation generation of probability profiles for specific-sequence macromolecules with long-range correlations, *Biopolymers,* 13, 1859, 1974.
192. **Lacombe, R. and Simha, R.,** Detailed balancing approach to disordered copolymeric Ising chains, *J. Chem. Phys.,* 58, 1043, 1973.
193. **Beck, E., Sommer, R., Auerswald, E. A., Kurz, Ch., Zink, B., Osterburg, G., Schaller, H., Sugimoto, K., Sugisaki, H., Okamoto, T., and Takanami, M.,** Nucleotide sequence of bacteriophage fd DNA, *Nucleic Acid Res.,* 5, 4495, 1978.
194. **Vologodskii, A. V. and Frank-Kamenetskii, M. D.,** Theoretical melting profiles and denaturation maps of DNA with known sequence: fd DNA, *Nucleic Acid Res.,* 5, 2547, 1979.
195. **Tong, B. Y. and Battersby, S. J.,** Comparison of theoretical denaturation maps of ϕX174 and SV40 with their gene maps, *Nucleic Acid Res.,* 6, 1073, 1979.
196. **Vournakis, J. N., Poland, D., and Scheraga, H. A.,** Anticooperative interactions in single-strand oligomers of deoxyriboadenylic acid, *Biopolymers,* 5, 403, 1967.
197. **Belintsev, B. N., Vologodskii, A. V., and Frank-Kamenetskii, M. D.,** Influence of base sequence on the stability of the double helix of DNA, *Mol. Biol. (Moscow),* 10, 764, 1976.
198. **Tong, B. Y. and Leung, M. L.,** Correlation between percentage guanine-cytocin content and melting temperature of DNA, *Biopolymers,* 16, 1223, 1977.
199. **Arnott, S. and Selsing, E.,** Structures for the polynucleotide complexes Poly(dA)-poly(dT) and Poly(dT)-poly(dA)-poly(dT), *J. Mol. Biol.,* 88, 509, 1974.
200. **Selsing, E., Wells, R. D., Early, T. A., and Kearns, D. R.,** Two contiguous conformations in a nucleic acid duplex, *Nature,* 275, 249, 1978.
201. **Domingo, E., Sabo, D., Taniguchi, T., and Weissmann, C.,** Nucleotide sequence heterogeneity of an RNA phage population, *Cell,* 13, 735, 1978.
202. **Sanger, F., Air, G. M., Barrell, B. G., Brown, N. L., Coulson, A. R., Fiddes, J. C., Hutchison, C. A., III, Slocombe, P. M., and Smith, M.,** Nucleotide sequence of bacteriophage ϕX174, *Nature,* 265, 687, 1977.
202b. **Sanger, S., Coulson, A. R., Freedman, T., Air, G. M., Barrell, B. G., Brown, N. L., Fiddes, J. C., Hutchinson, C. A., III, Slocombe, P. M., and Smith, M.,** The nucleotide sequence of bacteriophage ϕX174, *J. Mol. Biol.,* 125, 225, 1978.
203. **Wartell, R. M.,** The helix-coil transition of poly(dA)·poly(dT) and poly(dA-dT)·poly(dA-dT), *Biopolymers,* 11, 745, 1972.
204. **Borer, P., Dengler, B., Tinoco, I., Jr., and Uhlenbeck, O. C.,** Stability of ribonucleic acid double-stranded helices, *J. Mol. Biol.,* 86, 843, 1974.
205. **Patel, D. J. and Hilberts, C. W.,** Proton nuclear magnetic resonance investigation in double stranded dApTpGpCpApT in H_2O solution, *Biochemistry,* 14, 2651, 1975.
206. **Scheffler, I. E., Elson, E. L., and Baldwin, R. L.,** Helix formation by dAT oligomers. I. Hairpin and straight chain helices, *J. Mol. Biol.,* 36, 291, 1968.
207. **Scheffler, I. E., Elson, E. L., and Baldwin, R. L.,** Helix formation by d(TA) oligomers. II. Analysis of the helix-coil transition of linear and circular oligomers, *J. Mol. Biol.,* 48, 145, 1970.
208. **Klump, H. and Ackerman, T.,** Experimental thermodynamics of the helix-random coil transition. IV. Influence of the base composition of DNA on the transition enthalpy, *Biopolymers,* 10, 513, 1971.
209. **Privalov, P. L., Ptitsyn, O. B., and Birshtien, T. M.,** Determination of stability of the DNA double helix in an aqueous medium, *Biopolymers,* 8, 559, 1969.
210. **Shiao, D. D. F. and Sturtevant, J. M.,** Heats of thermally induced helix-coil transition of DNA in aqueous solution, *Biopolymers,* 12, 1829, 1973.
211. **Krakauer, H. and Sturtevant, J. M.,** Heats of the helix-coil transition of the poly A-poly U complexes, *Biopolymers,* 6, 491, 1968.
212. **Porschke, D., Uhlenbeck, O. C., and Martin, F. H.,** Thermodynamics and kinetics of the helix-coil transition of oligomers containing GC base pairs, *Biopolymers,* 12, 1313, 1973.
213. **Vedenov, A. A., Dykhne, A. M., and Frank-Kamenetskii, M. D.,** The helix-coil transition in DNA, *Sov. Phys.,* 14, 715, 1972.
214. **Rolfe, R. and Meselson, M.,** The relative homogeneity of microbial DNA, *Proc. Natl. Acad. Sci. U.S.A.,* 45, 1039, 1959.
215. **Sueoka, N., Marmur, J., and Doty, P.,** Heterogeneity in deoxyribonucleic acids. II. Dependence of the density of deoxyribonucleic acids on guanin-cytosin content, *Nature,* 183, 1429, 1959.
216. **Sueoka, N.,** On the genetic basis of variation and heterogeneity of DNA base composition, *Proc. Natl. Acad. Sci. U.S.A.,* 48, 582, 1962.
217. **Freese, E.,** On the evolution of the base composition of DNA, *J. Theor. Biol.,* 3, 82, 1962.
218. **Yanofsky, C., Cox, E. C., and Horn, V.,** The unusual mutagenic specificity of an *E. coli* mutator gene, *Proc. Natl. Acad. Sci. U.S.A.,* 55, 274, 1966.

219. Cox, E. C. and Yanofsky, C., Altered base ratios in the DNA of an *Escherichia coli* mutator strain, *Proc. Natl. Acad. Sci. U.S.A.*, 58, 1895, 1967.
220. Elton, R. A., Theoretical models for heterogeneity of base composition of DNA, *J. Theor. Biol.*, 45, 533, 1974.
221. Champoux, J. J. and Hogness, D. S., The topography of λ-DNA: poly rG binding sites and base composition, *J. Mol. Biol.*, 71, 383, 1972.
222. Yamagishi, H. and Takahashi, I., Heterogeneity in nucleotide composition of *Bacillus subtilis* DNA, *J. Mol. Biol.*, 57, 369, 1971.
223. Valenzuela, P., Venegas, A., Weinberg, F., Bishop, R., and Rutter, W. J., Structure of yeast phenylalanine-t RNA genes: an intervening DNA, *Proc. Natl. Acad. Sci. U.S.A.*, 75, 190, 1978.
224. Jovin, T. M., Recognition mechanisms of DNA-specific enzymes, *Annu. Rev. Biochem.*, 45, 889, 1976.
225. Brahms, S., Brahms, J., and Van Holde, K. E., Nature of conformational changes in poly[d(A-T)·d(A-T)] in the premelting region, *Proc. Natl. Acad. Sci. U.S.A.*, 73, 3453, 1976.
226. Pohl, F., Jovin, T. M., Baehr, W., and Holbrook, J. J., Ethidium bromide as a cooperative effector of a DNA structure, *Proc. Natl. Acad. Sci. U.S.A.*, 69, 3805, 1972.
227. Von Hippel, P. H. and McGhee, J. D., DNA-protein interactions, *Annu. Rev. Biochem.*, 41, 231, 1972.
228. Skalka, A., A method for the breakage of DNA and resolution of the fragments. I, in *Methods in Enzymology*, Vol. 21 (Part D), Grossman, L. and Moldave, K., Eds., Academic Press, New York, 1971, 341.
229. Younghusband, H. B. and Inman, R. B., The electron microscopy of DNA, *Annu. Rev. Biochem.*, 43, 605, 1974.
230. Inman, R. B., Denaturation mapping of DNA, *Methods in Enzymol.*, E29, 451, 1973.
231. Birnstiel, M. L., Chipchase, M., and Speirs, J., The ribosomal RNA cistrons, *Prog. Nucleic Acid Res.*, 11, 351, 1971.
232. Hoff, A. and Blok, J., The influence of single-strand breaks on the kinetics of denaturation of DNA, *Biopolymers*, 9, 1349, 1970.
233. Higuchi, S. and Tsuboi, M., The effect of polyamines on the melting profile of polyriboadenylic acid plus polyribouridilic acid complexes in solution, *Bull. Chem. Soc. Jpn.*, 39, 1886, 1965.
234. Gotoh, O., Wada, A., and Tada, M., Base and base sequence specificity of binding of 4-hydroxy aminoquinoline 1-oxide to DNA, *Gann*, 69, 61, 1978.
235. Karataev, G. I., Permogorov, V. I., Vologodskii, A. V., and Frank-Kamenetskii M. D., Denaturation maps of DNA: experimental and theoretical maps of X174 DNA, *Nucleic Acid Res.*, 5, 2493, 1978.
236. Scheffler, I. E. and Sturtevant, J. M., Thermodynamics of the helix-coil transition of the alternating copolymer of deoxyadenylic acid and deoxythymidylic acid, *J. Mol. Biol.*, 42, 577, 1969.
237. Hogan, M., Dattagupta, N., and Crothers, D. M., Transmission of allosteric effects in DNA, *Nature*, 278, 521, 1979.
238. Staynov, D. Z., Thermal denaturation profiles and the structure of chromatin, *Nature*, 264, 522, 1976.